Comparison of Average Female and Male Active HBM Responses in Whole-Sequence Frontal Crash Simulations

Johan Iraeus, Ekant Mishra, Jonas Östh

Abstract Active human body models (HBMs) are important enablers for the simulation of occupant kinematics in pre-crash manoeuvres in whole-sequence crash scenarios. Pre-crash kinematics as well as injury risks have been shown to vary with sex. In this study, an average-sized female version (F50) of the active M50 SAFER HBM was developed using parametric mesh morphing, complemented with scaling of the muscle cross-sectional area. The active F50 model was validated with respect to volunteer pre-crash kinematics in braking and evasive turning manoeuvres, for two different belt systems (standard/pre-tensioned). Overall, the active F50 model predictions were slightly on the compliant side, compared to the volunteer test data. However, quantitatively using the CORA method, the active F50 model showed good biofidelity (0.81/0.89) for the pre-crash braking manoeuvre and fair biofidelity (0.60/0.75) for the evasive turning manoeuvre. Whole-sequence, combined, pre-crash and in-crash simulations were run with the active F50 and M50 models. They revealed some differences between the models, for which the active F50 model showed lower upper body forward displacements, and higher pelvis displacements, for two crash configurations and belt systems, compared to the active M50 model. Overall, however, the differences were small between the two HBMs.

Keywords Active muscle, average female, human body model, finite element, postural control.

I. INTRODUCTION

Vehicle safety systems are continuously improving, and modern vehicles offers a high level of protection for vehicle occupants [1]. Research has indicated some differences in the injury risk related to population variations, such as age and sex of the occupant [1-3]. Some of these differences can be attributed to dissimilarities in vehicles and crashes [4], but the ability to include effects of physiological differences in the occupant population in crash simulation could help improving vehicle safety even further.

Further, autonomous crash avoidance systems, through braking and steering manoeuvres, have the potential to reduce crash severities and prevent crashes altogether [5-8]. However, in the case a crash is inevitable, the avoidance manoeuvre may alter the occupant pre-crash position and muscle activation [9-11], which might influence the injury risk in the subsequent crash [12-14]. Some studies have analysed the effect of sex on pre-crash kinematics, but with mixed results [9,10,15-18]. Even if sex has been shown to be a significant predictor for occupant kinematics in some evasive manoeuvres, this effect is small compared to the overall population variability [17-19]. Quantifying the effect of population variability is important to ensure that countermeasures are robust.

There are several anatomical differences which might explain some of the sex-related variability in pre-crash manoeuvres. On average, females have more adipose and less muscle tissue, resulting in lower muscle strength than average males [20,21]. This is more pronounced in upper body muscles and for concentric rather than eccentric contractions due to lower muscle mass and fewer type II fibres, rather than a lower voluntary activation level [22].

Virtual Finite Element (FE) Human Body Models (HBMs) offer some advantages over crash test dummies, as FE HBMs can be equipped with active muscles and postural control algorithms required to accurately predict pre-crash kinematics. At the same time, the high level of anatomical detail enables analysis of injury risk on the tissue level. In addition, HBMs can be morphed to represent a wide range of the population [23-25]. Examples of contemporary HBMs are; the Total Human Model for Safety (THUMS) [26], the Global Human Body Model Consortium (GHBMC) [27], the SAFER HBM [28], and the VIVA+ HBM [29]. Some of these models include active

J. Iraeus, PhD, (e-mail: johan.iraeus@chalmers.se, tel. +46 31 772 1366) is a researcher at Chalmers University of Technology, Sweden. E. Mishra is a Research Engineer at Autoliv Research, Vårgårda, Sweden. J. Östh, PhD, is a Technical Expert for Human Body Modelling at the Volvo Cars Safety Centre, Gothenburg, Sweden and an Adjunct Associate Professor at Chalmers University of Technology, Sweden. All authors are associated with SAFER – Vehicle and Traffic Safety Centre at Chalmers in Sweden.

muscles with postural control and have been validated for pre-crash kinematics [30-32]. However, the validations have so far focused on HBMs representing an average male, with the exception of two models that were validated for active F05 HBMs [33,34].

There is evidence that muscle activation can influence the injury risk in the crash phase. In some studies, pre-defined muscle activation patterns, for example from Electromyography (EMG) measurements, have been used to study the influence on injury risk [35-39], and in some more recent studies, muscle activation based on postural feedback control has been used [30,40,41]. The results are mixed, in some cases muscle activation increases the injury risk, while in other cases the injury risk decreases. None of these studies evaluated if sex influences the outcome.

Thus, as an initial step to address the lack of validated active HBMs representing the whole population, the first aim of the study was to develop an average sized active female HBM and validate its pre-crash kinematics. The second aim was to compare this model to a baseline average sized active male HBM in whole-sequence frontal crash simulations.

II. METHODS

The SAFER HBM v10 50th percentile male active (M50) model was morphed to an average, 50th percentile, active female (F50) using a parametric morphing method, accounting for sex, age, stature, and Body Mass Index (BMI). The active F50 HBM was validated with respect to front seat passenger occupant kinematics responses in pre-crash braking and evasive turning manoeuvres using an objective correlation method (CORA). The active F50 HBM and the baseline active M50 HBM were then compared in whole-sequence pre-crash braking and frontal crash simulations, as well as an evasive turning manoeuvre followed by an oncoming crash.

All simulations were carried out using LS-DYNA MPP R9.3.1 (ANSYS/LST, Livermore, CA), HBM pre-processing and positioning with ANSA (Beta CAE Systems, Luzern, Switzerland) and PRIMER (OASYS Ltd., Sollihull, UK).

Active F50 HBM Modelling

The baseline HBM was the SAFER HBM version 10 [28] which is an active M50 occupant model of 1.75 m stature with a mass of 77 kg. This model includes active muscle postural control for the neck and trunk, modelled using an Angular Position Feedback (APF) control method [32,41,42]. The active M50 baseline model has previously been validated in braking, lane change and combined manoeuvres [32]. In addition, the model has been subjected to extensive in-crash kinematics and injury prediction validation [28,43-45].

The baseline active M50 HBM was morphed to an active F50 HBM using the parametric HBM morphing method described in [23]. The target F50 parameters were 45 years of age, a stature of 1.62 m and a BMI of 23.6 [46]. More details on the morphing method and validation of in-crash kinematics and injury risk of morphed SAFER HBMs can be found in [47]. After morphing, the contacts of the active F50 model were fully depenetrated, and element quality was checked to be on par with the active M50 model [28].

As previous studies indicate that the sex-related difference in muscle strength is related to difference in muscle mass rather than voluntary activation [22], the cross-sectional muscle area was updated to create the active F50 HBM. The muscle area, and thus the strength of the active F50 HBM was adjusted to 63% of the male baseline HBM, by scaling the Physiological Cross-Sectional Area (PCSA) of the muscle elements based on the difference between males and females in literature sources [48-50]. The controller settings, including the Proportional – Integral – Derivative (PID) gains, were not modified.

Active F50 HBM Validation

The active F50 HBM was validated based on two sets of volunteer experiments which included kinematics, seatbelt forces, and muscle activation data normalised to the volunteers' Maximum Voluntary Contraction (MVC). The first set of volunteer experiments represented an autonomous pre-crash braking event in the passenger seat of a mid-size passenger car [9]. The second set of volunteer experiments represented an evasive turning manoeuvre consisting of an initial right turn followed by a left turn in the passenger seat of a mid-size passenger car [51,52]. Two types of seatbelt configurations, a standard seatbelt, and an Electrical Reversible Retractor (ERR) seatbelt in which a 170 N tension force was applied 200 ms prior to braking initiation were used.

Averaged pulses, derived from the experiments, were used for the braking and evasive turning simulations as shown in Fig. 1 [9,51]. For the braking scenario, t0 was defined as the time when vehicle acceleration was 5% of the peak value, while for the evasive turning scenario, manoeuvre initiation was defined as t0 [9,51]. In the

simulations with the ERR pre-tensioned seatbelt, the retractor was activated at 640 ms (257 ms before t0) for braking and at 470 ms (280 ms before t0) for evasive turning [32]. The total simulation time for all validation simulations also included the time for positioning the HBM on the seat. The seat model used for the validation simulations was a generic deformable seat model based on a production seat [53]. Only gravity loading was applied from 0–250 ms while the head and the first thoracic vertebra (T1) were brought to equilibrium with a prescribed rearward displacement of 8 mm similar to the procedure in [32]. Muscle activation was added to the gravity loading between 250–750 ms, with the reference position time set as 250 ms.

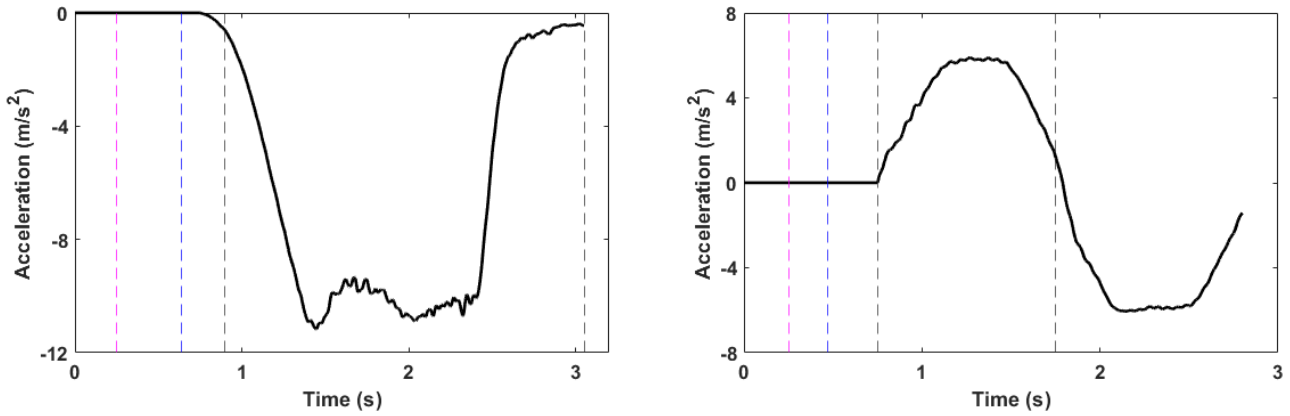

(a) Braking (b) Evasive turning

Fig. 1. Average braking and evasive turning pulses from the volunteer experiments. The black dashed lines show the CORA evaluation intervals for the simulations, the blue dashed lines show the retractor activation times for the ERR, and the magenta dashed lines show the start of the muscle dynamics. Gravity loading started at 0 s.

The model validation consisted of a total of four simulations: pre-crash braking (with and without ERR), and evasive turning (with and without ERR). Head translations, head rotations, first thoracic vertebrae (T1) translations, and forces on the shoulder and lap belts were compared to the experimental results to validate the model. The muscle activations of the sternocleidomastoid (SCM), cervical paravertebral muscles (CPVM)/semispinalis capitis (SCap), lumbar paravertebral muscles (LPVM)/erector spinae (longissimus), and rectus abdominis (RA) muscles were compared with the normalised muscle activation data from the experiments.

The predicted kinematics and seatbelt forces were compared to the volunteer data to evaluate the biofidelity by an objective correlation method (CORA) using the CORAplus 4.0.5 software [54]. The average volunteer responses were used as the reference, with the average ±1 and ±2 Standard Deviations (SD) being used as the inner and outer corridors respectively [32]. The evaluation interval was between t0 and the end of the simulation for the pre-crash braking scenario and between t0 and the end of the first phase for the evasive turning scenario. Table A1 in the Appendix contains the evaluation settings used for CORA. The CORA ratings were classified as excellent (>0.94), good (>0.80), fair (>0.58), or poor (<=0.58), for easier interpretation, following the method described in [55].

Comparison of Active F50 and M50 HBMs in Whole-Sequence Crash Simulations

Two types of whole-sequence crashes were simulated with the active F50 and M50 models, Table I. The first included only longitudinal vehicle kinematics, in the form of a Full-Frontal Rigid Barrier (FFRB) pulse from a 56 km/h impact. For some simulations, a 6 km/h velocity reduction due to pre-crash braking was accounted for by reducing the FFRB pulse severity to a 50 km/h impact. The second sequence consisted of a high-severity oncoming crash with 50% overlap for two cars, each with an initial velocity of 50 km/h [8], with and without an evasive turning manoeuvre to the right. The pre-crash braking was modelled with a constant jerk of 55 m/s3 for 200 ms to reach an acceleration of 11 m/s2 [56]. The acceleration was kept constant at this level for another 59 ms, corresponding to a velocity reduction of 6 km/h. The evasive right turning manoeuvre was modelled as the mirrored 6 m/s2 lateral acceleration from an experimentally recorded left turn [51], for 700 ms, corresponding to a lateral movement for the car of 1 m.

TABLE I
WHOLE-SEQUENCE CRASH SIMULATION MATRIX.

Simulation	HBM	Postural Control	Pre-crash Manoeuvre	ERR	Crash Pulse	Pre-crash Duration (ms)	Crash Duration (ms)	Total Simulation Time (ms)
1	M50	Active	No	No	FFRB 56 km/h	0	150	450
2	F50	Active	No	No	FFRB 56 km/h	0	150	450
3	M50	Active	Braking	No	FFRB 50 km/h	259	150	709
4	F50	Active	Braking	No	FFRB 50 km/h	259	150	709
5	M50	Active	Braking	Yes	FFRB 50 km/h	259	150	709
6	F50	Active	Braking	Yes	FFRB 50 km/h	259	150	709
7	M50	Passive	No	No	FFRB 56 km/h	0	150	450
8	F50	Passive	No	No	FFRB 56 km/h	0	150	450
9	M50	Active	Braking	No	FFRB 56 km/h	259	150	709
10	F50	Active	Braking	No	FFRB 56 km/h	259	150	709
11	M50	Active	Braking	Yes	FFRB 56 km/h	259	150	709
12	F50	Active	Braking	Yes	FFRB 56 km/h	259	150	709
13	M50	Active	No	No	Oncoming	0	120	420
14	F50	Active	No	No	Oncoming	0	120	420
15	M50	Active	Turn	No	Oncoming	700	120	1120
16	F50	Active	Turn	No	Oncoming	700	120	1120
17	M50	Active	Turn	Yes	Oncoming	700	120	1120
18	F50	Active	Turn	Yes	Oncoming	700	120	1120

The whole-sequence crashes were simulated in a FE occupant compartment simulation model of a mid-size Sports Utility Vehicle consisting of a rigid body in white with deformable interior (seat, instrument panel etc.). The HBMs were positioned using the Marionette method [57] in the passenger seat, in an upright posture with the arms close to the body and the hands close to the legs (Fig. A 10). The seat was in its lowest position, and at mid fore-aft travel length, with a seat-back angle of 25° for both HBMs who were positioned with their H-points matching that of an SAE-manikin. Due to the shorter legs of the F50 HBM, the feet were resting with the heel on the carpet compared with those of the M50 which were on the footrest. A passenger airbag deploying upward from the instrument panel was used in the crash phase, in combination with a three-point standard seatbelt with a pyro-technical pretensioner and a single-stage load-limiter. Additionally, an ERR with a nominal force level of 200 N was modelled and used as an intervention in the pre-crash phase of some whole-sequence simulations (TABLE I). For all simulations, a 300 ms initialisation phase was included to settle the HBM in the seat and initialise the postural control. At the start of the crash-phase, the muscle activations were frozen and held constant [41]. For the simulations with the *passive* HBM (TABLE I), the postural control was turned off after the initialisation phase to provide the same initial conditions at the start of the crash phase for all simulations. All displacements were calculated relative to the position after the 300 ms initialisation phase.

III. RESULTS

A comparison of the distributions of Jacobian, Warping and Aspect ratio element quality criteria for the solid elements of the active F50 and M50 models showed that the morphing process resulted in only a small degradation of element quality criteria, Fig. A 1. This can be seen as a shift in the distributions. Both models were robust, as no simulations, either pre-crash validation or whole-sequence simulations terminated prematurely. The resulting active F50 model can be seen alongside the base active M50 model, for comparison, in Fig. 2.

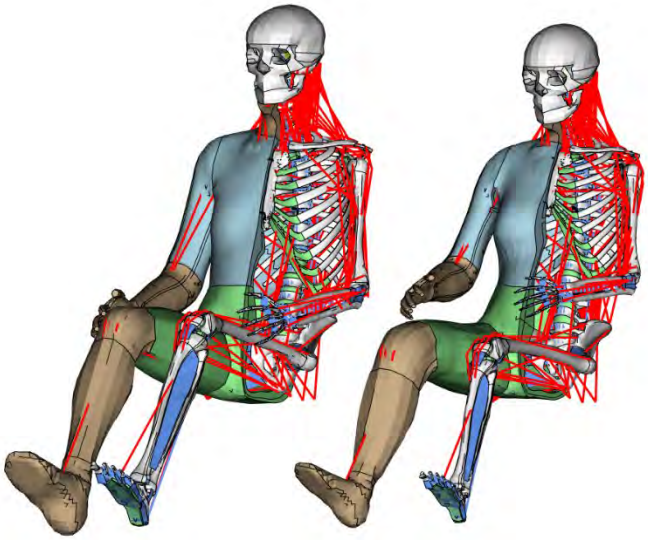

Fig. 2. Left: The baseline Active M50 SAFER HBM. Right: The morphed active F50 SAFER HBM.

Active F50 HBM Validation: Pre-Crash Braking

The kinematics from the pre-crash braking simulations were similar to the kinematics observed in the volunteer study and were, for most of the pre-crash duration, within the ±1 SD corridor for both the standard and the ERR seatbelts, although closer to the +1 SD curve (Fig. 3). However, oscillations were observed in the HBM head rotation (mainly visible in the Head Y rotation signal), which was not found in the average volunteer response. The forces in the shoulder and lap belts, as illustrated in Fig. A 2 in the Appendix, were also within the ±1 SD corridor except for the initial peak for the shoulder belt force in the simulation with the standard seatbelt.

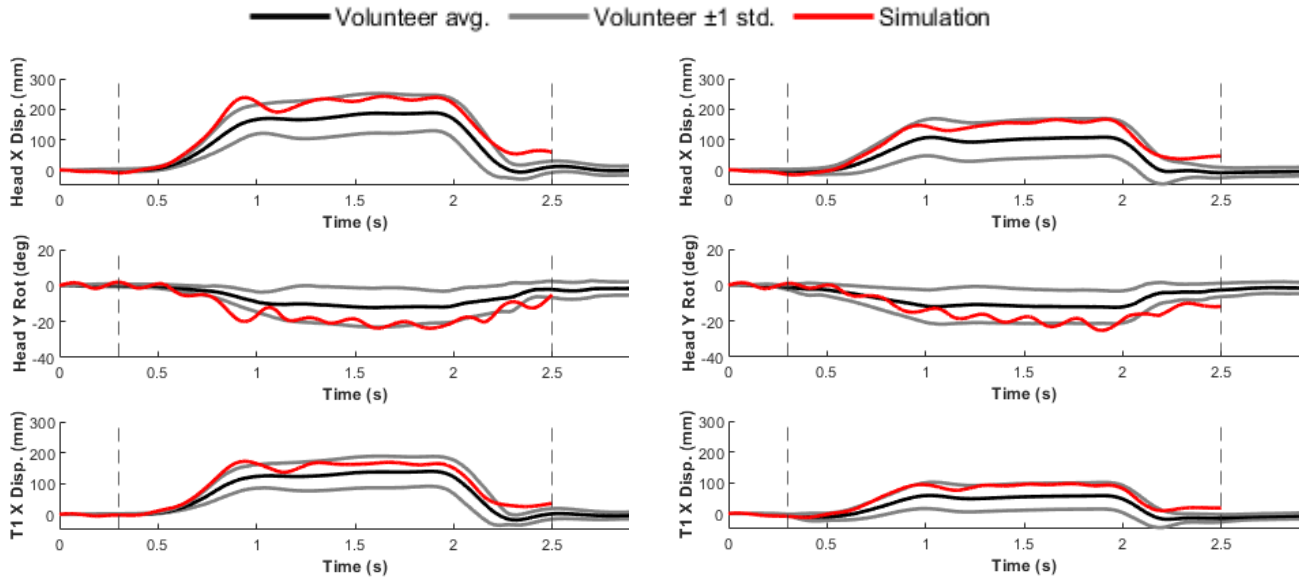

(a) Standard seatbelt (b) ERR seatbelt

Fig. 3. Kinematics for pre-crash braking simulations with (a) standard seatbelt and (b) ERR seatbelt. The black curves show average F50 volunteer response [9], grey curves show average ±1 SDs, and the red curves show active F50 HBM response. The vertical dashed lines show the evaluation interval.

The SCM, LPVM, and RA muscle activations were mostly within the ±1 SD corridor comparing well to the volunteer data (Fig. A 4). On the other hand, higher levels of CPVM muscle activation were observed in the simulations. Muscle activation levels in the simulation with the ERR seatbelt were slightly lower, more consistent with the muscle activation levels observed in the volunteer data (Fig. A 5).

Active F50 HBM Validation: Evasive Turning

For the evaluated kinematics, the active F50 HBM predicted higher displacements compared to the volunteers in the evasive turning scenario (Fig. 4). However, the model response in the lateral (Y) direction, which is dominating the response in the evasive turning manoeuvre, was close to the +1 SD curve, showing that the model prediction was on the compliant side. Moreover, within the model evaluation interval (indicated with vertical dashed lines), the kinematics predicted in the simulation with the ERR seatbelt showed better correlation with the volunteer data.

Shoulder and lap belt forces matched well with the average volunteer response within the evaluation interval, as depicted in Fig. A 3 in the Appendix. However, the predicted lap belt force in the simulation with the standard seatbelt was entirely outside the SD corridor.

Although similar in shape, all predicted muscle responses compared poorly with the volunteer EMG data, showing much higher activation levels, (Fig. A 6 and Fig. A 7). The active F50 HBM with the ERR seatbelt produced lower muscle activation, consistent with the volunteer data.

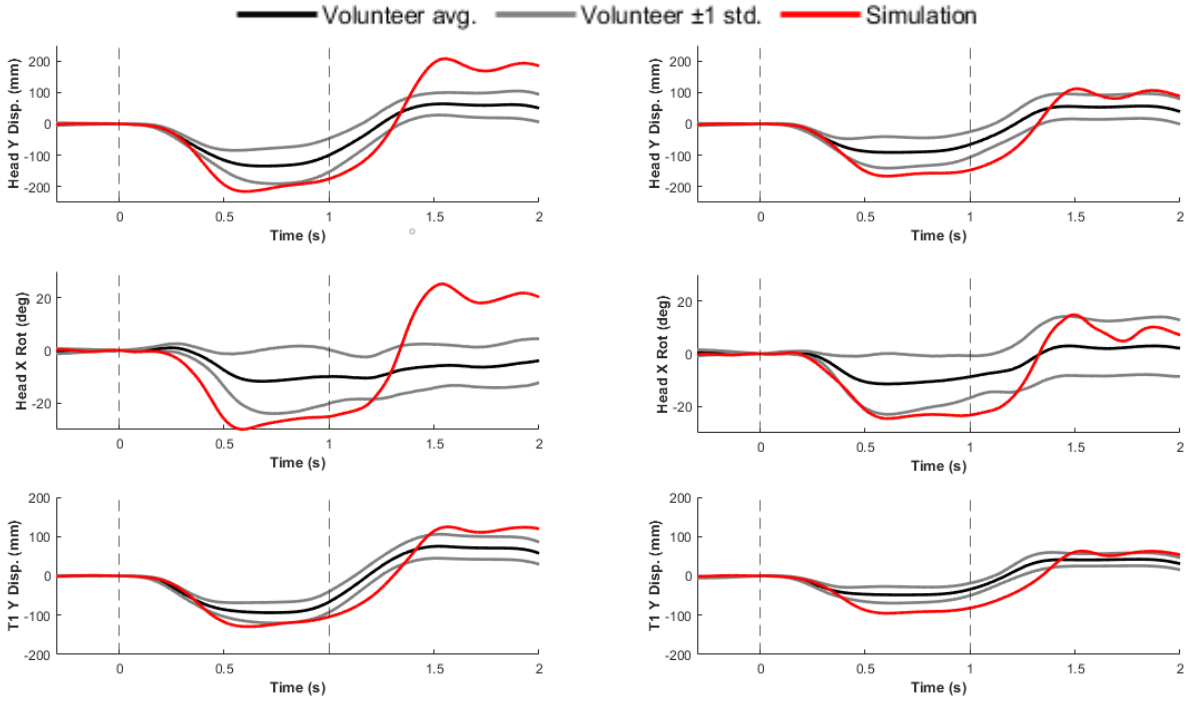

(a) Standard seatbelt (b) ERR seatbelt

Fig. 4. Head and T1 kinematics for the evasive turning simulations with (a) standard seatbelt and (b) ERR seatbelt. The black curves show average F50 volunteer response [52], grey curves show average ±1 SDs, and the red curves show active F50 HBM response. The vertical dashed lines show the evaluation interval.

Active F50 HBM Validation: CORA Ratings

Fig. 5 below shows the individual CORA ratings for head and T1 displacements, shoulder and lap belt forces, and the overall ratings per load case. CORA ratings indicate a good correlation between the active F50 and the average female volunteer response for the pre-crash braking scenario with both the standard (average CORA 0.81) and the ERR seatbelts (average CORA 0.89). There were no substantial differences in the individual signal ratings for this scenario.

However, for the evasive turning scenario, the CORA ratings were lower, indicating a fair correlation with both the ERR and the standard seatbelts (average CORA 0.75 and 0.60, respectively). The lap belt force showed poor correlation with volunteer data in the standard seatbelt load case.

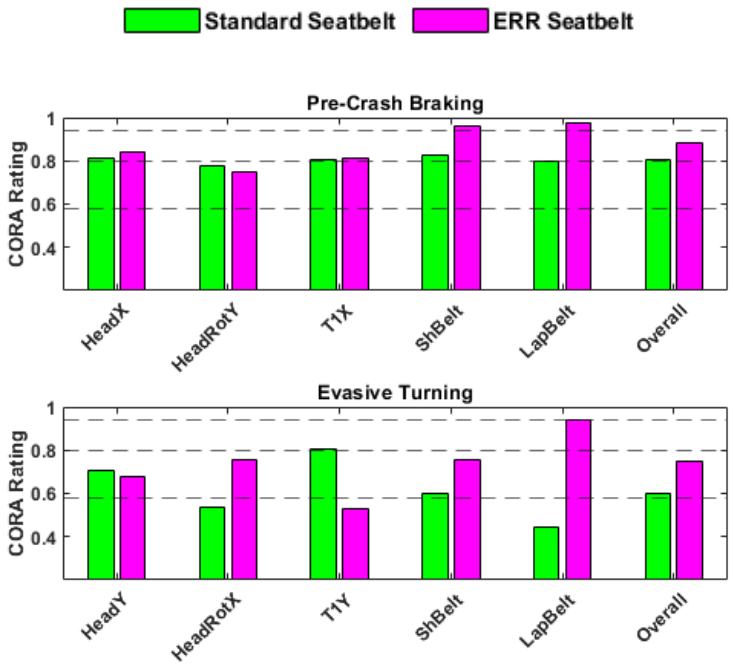

Fig. 5. CORA ratings for the pre-crash braking and evasive turning simulations. The dashed lines indicate the level of correlation, excellent (>0.94), good (>0.80), and fair (>0.58).

Comparison of Active F50 and M50 HBMs in Whole-Sequence Crash Simulations

For both pre-crash manoeuvres, the active M50 and F50 HBMs moved away from their initial positions due to the manoeuvre. For the pre-crash braking without the ERR (Simulations 3 and 4), Fig. 6, the HBM's upper body moved downward and forward, and was still moving forward at the start of the crash phase. The active F50 HBM had similar head forward displacement, 154 mm at the start of the crash phase, to the active M50 HBM (153 mm), while the T1 displacement was the same for both HBMs (118 mm), Fig. 7. For the evasive turning pre-crash manoeuvre (Simulations 15 and 16), with a longer duration, the active F50 HBM did have time to recover some of the pre-crash induced lateral displacement, Fig. 6. The peak lateral head displacement was higher at 231 mm for the active F50 HBM compared with the active M50's 150 mm, Fig. 7. For the pre-crash manoeuvres with ERR (Simulations 4, 5, 17 and 18) the ERR reduced the displacements for both HBMs. In the pre-crash braking, the chest of the active F50 HBM was somewhat more constrained than the active M50 because of the ERR activation, with a peak forward displacement of 53 mm compared with 59 mm, respectively. For the turning evasive manoeuvre, the ERR reduced the lateral displacements, to 151 mm and 94 mm for the active F50 and M50 HBM's heads, respectively.

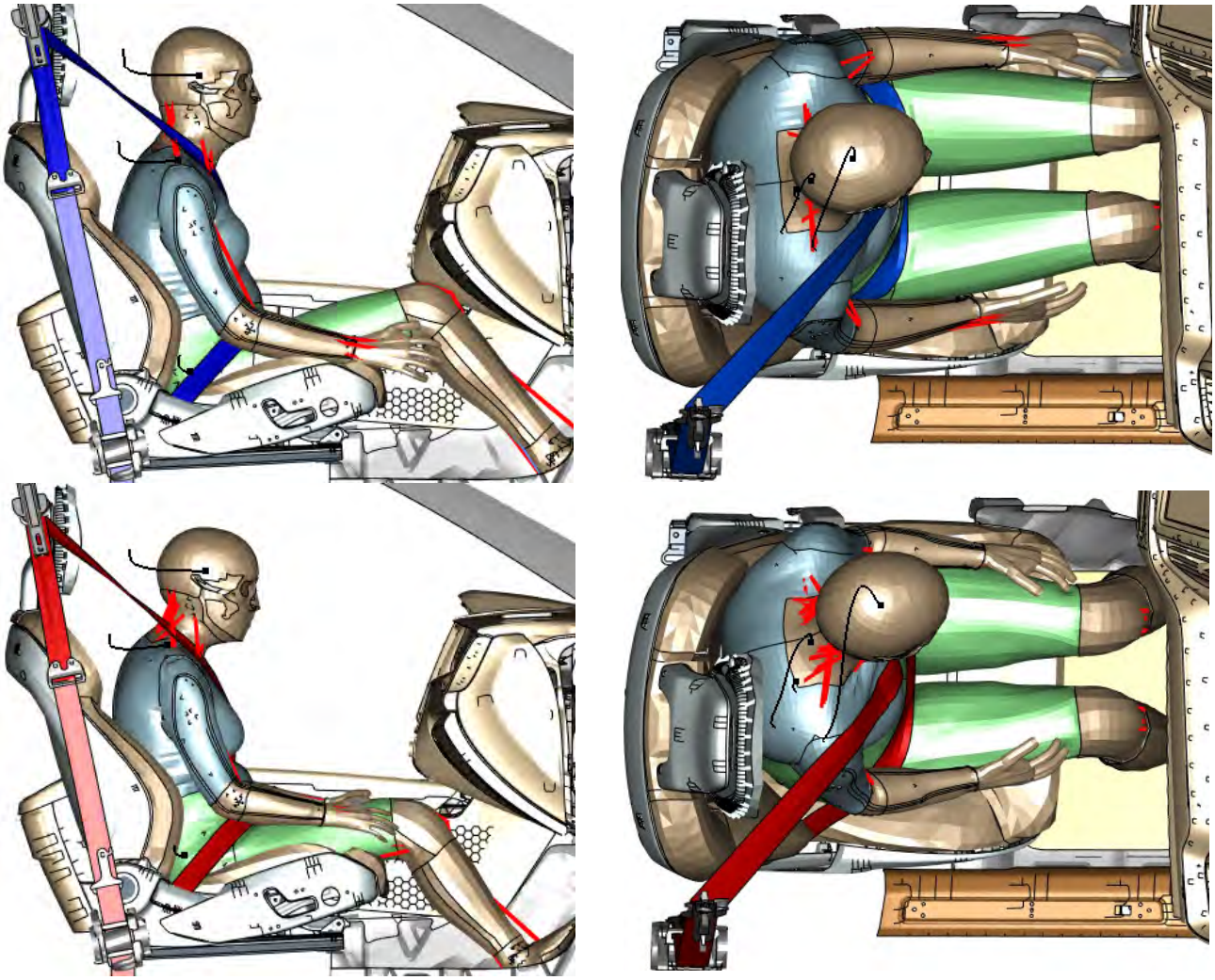

Fig. 6. Pre-crash kinematics at the start of crash in whole-sequence Simulations 3 and 4 with pre-crash braking, and 15 and 16 with the pre-crash turning evasive manoeuvre. Top row: Active M50 HBM. Bottom Row: active F50 HBM.

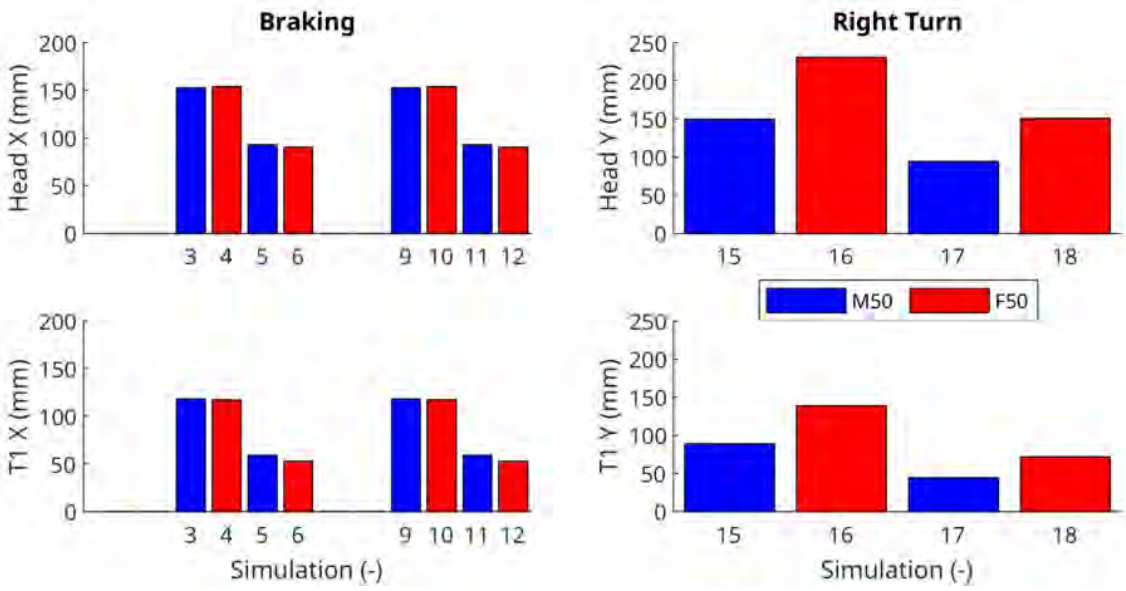

Fig. 7. Peak pre-crash head and first thoracic (T1) vertebra displacements. Left: Peak forward X displacements in the pre-crash braking simulations. Right: Peak inboard Y displacements in the turning evasive manoeuvres. Simulation 3, 4, 9, and 10 were for pre-crash braking without ERR, Simulations 5, 6, 11, and 12 pre-crash braking with ERR, while Simulations 15 and 16 were for turning without ERR and 17 and 18 turning with ERR.

The muscle activations, Fig. 8, at the end of the pre-crash braking phase, were highest in the cervical and lumbar extensor muscles, in particular the Splenius Capitis (SCap) for which it was 65/77 % and 74/67 % for the active M50 and F50 HBMs left/right side, respectively. The difference in which side had the highest muscle activation was due to a difference in the interaction with the shoulder belt, which acted higher up on the chest for the active F50 HBM. Except this minor difference, the magnitude of muscle activations was similar for both models in both the pre-crash manoeuvres and hence also in the subsequent crash phase simulations.

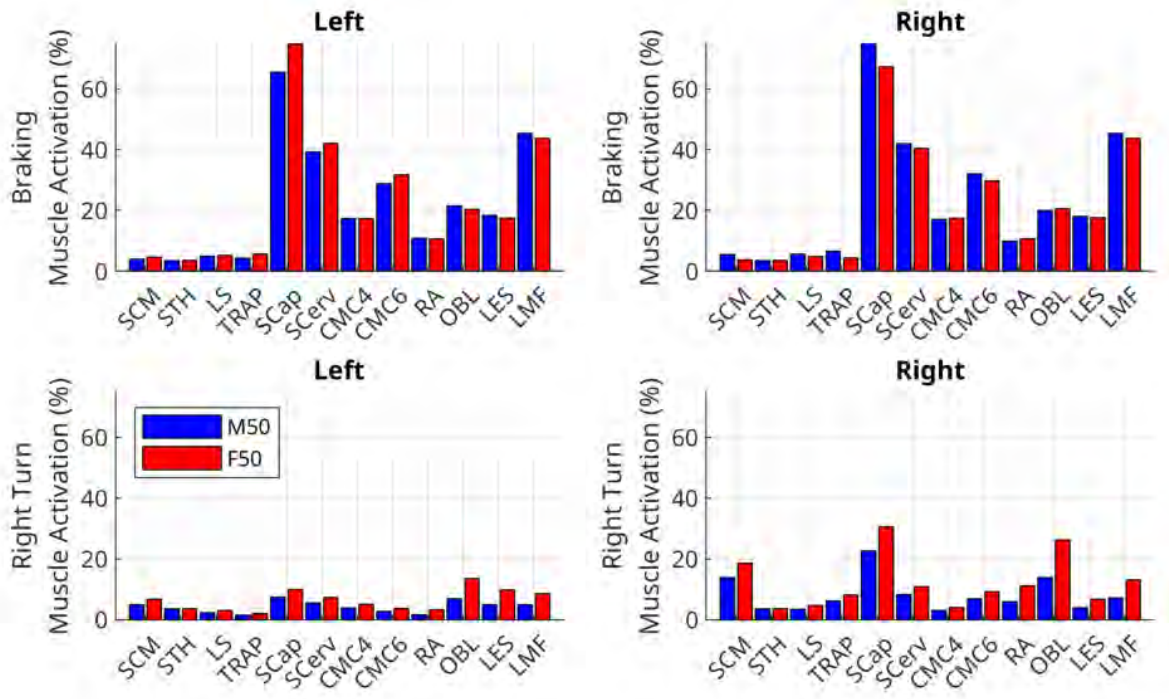

Fig. 8. Muscle activations at the end of the pre-crash phase for Simulations 3 and 4 (pre-crash braking) and Simulation 15 and 16 (evasive right turn). Muscle group abbreviations according to Fig. A 8 and Fig. A 9 in the Appendix.

For the crash phase of the whole-sequence simulations, for the FFRB 56 km/h crashes without any pre-crash intervention with both active (Simulation 1 and 2) and passive HBMs (Simulation 7 and 8) had similar peak forward X displacements that were 37 mm higher for the head and T1 for the active M50 HBM than for the F50 model, Fig. 9, Fig. A 15 and Fig. A 16 in the Appendix. At the same time, the active F50 HBM had higher sacrum displacements, due to more soft tissues in the pelvic area (Fig. A 18). For example, peak X displacements for the active M50 HBM in Simulation 1 were 526 mm, 426 mm, and 125 mm, for the head, T1 and sacrum, respectively, while for the active F50 HBM in Simulation 2 they were 489 mm, 397 mm, and 184 mm.

Even though the pre-crash braking intervention led to a more forward position at the start of the crash phase, it reduced overall peak forward displacements in the crash phase for the FFRB 56 km/h simulations with both pre-crash braking and pre-crash braking and ERR (Simulations 9–12), about 60 mm for the head forward displacement for both HBMs. Similarly, reducing the impact speed from 56 km/h to 50 km/h reduced the forward head displacement in the order of 85 mm for both HBMs, which can be seen when comparing the results of Simulations 1–2 to 3–4 (Fig. 9).

For the oncoming crashes, the forward head displacements were similar for all simulations (Simulations 13–18, Fig. 9), reaching approximately 520/480 mm for the head for the active M50/F50 HBMs, while some minor variations were noticed for the T1 and sacrum.

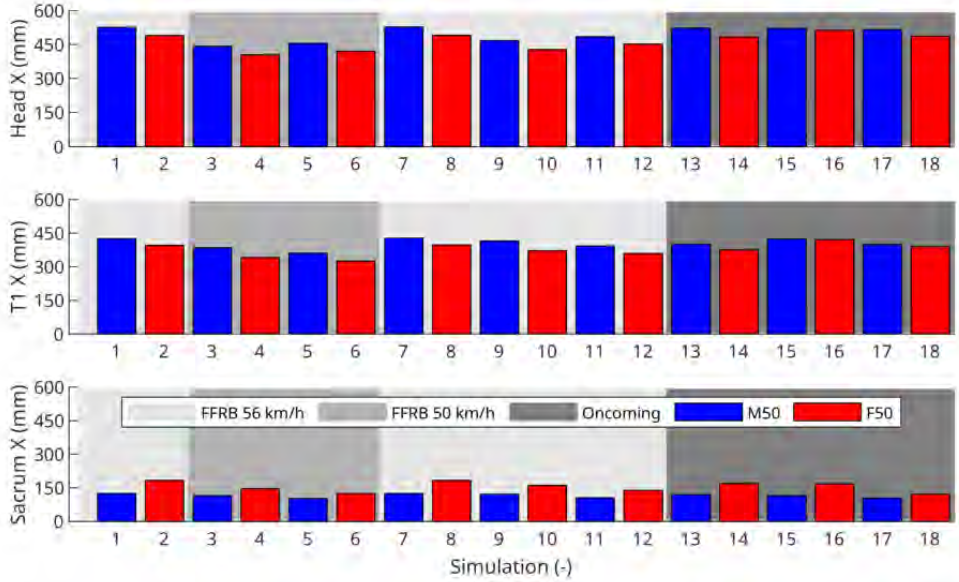

Fig. 9. Peak forward X displacements for the head, first thoracic (T1) vertebra and sacrum during the crash phase for all simulations.

IV. DISCUSSION

An average female HBM was created by morphing the average male SAFER HBM and scaling the muscle cross-sectional areas. The parametric morphing method used here [23], is based on several statistical regression models, controlling not only the outer shape [58], but also several skeletal bone geometries [59-61]. Sex, together with age, BMI, and height, are used as co-variates in the regression, meaning that sex-related differences in outer body shape as well as sex-related skeletal differences are accounted for. However, during the morphing process, only the FE nodes were moved, and therefore, the model properties defined in other ways were not updated. This includes for example, thickness of cortical bones modelled using shell elements, and material properties. While many studies have shown that neither cortical thickness nor bony material properties differ between equal-sized, young and middle-aged, males and females [62-64], it has also been shown that the properties of soft tissues like ligaments can differ [65]. This means that it is likely that the current version of the active F50 SAFER HBM have reasonable bony mechanical properties (related to the fracture risk), while future versions should consider updating soft tissue properties, which could influence the (pre-crash and in-crash) kinematics.

Previous studies have shown that the body composition differs between males and females, for which females have more fat tissue and males more muscle tissue, which results in males being on average stronger than females. The higher muscle strength is more pronounced in the upper body (which is the main focus of this study) and has been linked to greater muscle mass and type II fibres, rather than higher voluntary activation in males [22]. As a result, the modelling assumption was to only scale the female muscle PCSA to 63% of the male PCSA, leaving other muscle controller parameters unchanged.

The active F50 HBM was validated with respect to average female front seat passenger volunteer pre-crash kinematic data and seatbelt forces for two load cases: autonomous pre-crash braking and evasive turning. The model was able to reproduce the postural response of average female passengers in pre-crash braking, showing good biofidelity. However, for evasive turning manoeuvres, the model only showed fair biofidelity. There could be many reasons for this difference in biofidelity. The HBM interaction with the vehicle is more complex in the evasive turning compared to the braking load case. In the braking load case, the occupant's torso moves into and gets constrained by the shoulder belt. The modelling of the shoulder belt, including the resulting belt forces are well defined and simulation predictions correlate well to physical test results. However, in the evasive turning manoeuvre the torso is only partially constrained by the shoulder belt. For in-crash far-side loading, it has previously been shown that the shoulder belt to torso interaction lacks in biofidelity, meaning that the friction had to be artificially increased for that load case [28,66]. It is possible that for pre-crash load cases too, the shoulder belt interaction with the upper body lacks validity. In addition to the seatbelt, the torso is also constrained by the seat back bolsters and by the lumbar muscles. The modelling of the seat back bolsters has not

been validated to the same extent as the rest of the seat foam and could potentially have incorrect stiffness for lateral loading. Further, the lumbar controller might be less effective compared to the neck controller, as indicated by the head to T1 relative displacements in Fig. 3 and Fig. 4. The predicted head to T1 relative displacements match the volunteer results well (seeing as both head and T1 is about 50 mm above the average volunteer responses). This means that it is most likely the lumbar controller that lacks in biofidelity.

In both the braking and evasive turning load cases, the model response was close to the +1 SD envelope, meaning that the model's overall prediction was on the compliant side. The accurately captured belt forces (Fig A1 and A2) indicate that the net effect of the muscles was on the weaker side, mainly for the lumbar muscles, as discussed above. This could be due to lower muscle forces, because of smaller PCSA or lower muscle excitation, or unphysical muscle routing (point-to-point rather than an anatomical path) giving the muscles smaller lever arms. The PCSA of the active F50 model was scaled to 63% of the male PCSA, based on literature on neck muscles [48-50]. The other important muscle group for occupant precrash kinematic is the trunk muscles. Male to female scaling for the trunk muscles have been reported to be about 60-64% [22]. Thus, it was decided to use the neck scaling factor of 63% for the whole model. Therefore, it is also unlikely that the lower lumbar muscle forces are due to lower PCSA. As indicated by Fig A5 And Fig A6, the activation of the trunk muscles seems feasible, suggesting that the muscle routing might be causing the lower muscle forces. However, the validation results of the active F50 model can also be compared to the validation results for the active M50 active SAFER HBM reported in [32]. The active M50 model had CORA ratings of 0.81 and 0.82, respectively for the standard and pre-tensioned seatbelts, in pre-crash braking. In evasive turning, the active M50 model had CORA ratings of 0.78 and 0.84, for the standard and pre-tensioned seatbelts, respectively. Comparing the previous study active M50 study to the current study, the CORA ratings were comparable in the pre-crash braking load case. However, in the evasive turning load case, the CORA ratings of the active F50 model were lower. The predicted kinematics for the active M50 model agreed well to the average volunteer response, while in the current study the predicted kinematics for the active F50 model were on the compliant side (close to the +1 SD envelope). As the muscle routing is similar in the two models, this points away from the muscle routing hypothesis. The muscle excitement, which is controlled by the PID controller, is left to investigate. In addition to the controller gains, the controller also incorporates the neural delay. Females have been shown to have faster reaction times [67], so future updates of the feedback controller should investigate if retuning the PID gains, including updates of the neural delay for the active F50 HBM, can further improve the model predictability. It is possible that better correlation in the validation setup would be achieved by retuning of the controller gains, specifically for the female model, but the results of the validation here is promising for a population-based morphing approach as a relatively simple scaling gave a reasonably good validation response for the active F50 HBM. The active F50 HBM was also able to replicate the volunteer trend of lower muscle activations in the ERR seatbelt load case compared to the standard seatbelt.

Activating an ERR seatbelt could trigger a startle response in occupants, which was observed in the volunteer EMG data. However, like the active M50 HBM, the active F50 HBM was not able to reproduce this response [32,68]. The effect of a startle response was not implemented and investigated in the present study, but a possible approach would be to model it as a triangular impulse in the control signal to all muscles, as done in [41].

Both HBMs demonstrated their ability to simulate whole-sequence crashes. For the pre-crash braking simulations, only minor differences in occupant peak displacements were found in a comparison between the HBMs, most likely due to the short time span for the pre-crash braking (259 ms). During this short time, the head and torso of the occupants only have time to start moving, and their responses are close to that of a free-flying mass. For longer pre-crash braking simulations [41], a difference in forward displacements between the male and female HBMs could be expected. Nevertheless, both HBMs experienced reduced forward displacements due to the inclusion of an ERR function in the pre-crash braking simulations. For the right turn pre-crash event, larger changes stemming from the difference in anthropometry were found. The active F50 HBM has considerably higher inboard displacements due to the narrower width over the hips, leading to less support from the tunnel console and higher inboard peak head and T1 displacements.

Even though the pre-crash manoeuvres changed the occupants' position at the start of the crash phase, relatively small differences in peak forward position in the crash phase were found for all simulations (Fig. 9 and Fig. A 15 - Fig. A 17 in the Appendix). The active F50 HBM had relatively lower upper body peak forward displacements during crash than the active M50 HBM, due to its shorter stature and lower mass. In addition, the active F50 HBM had relatively greater lower body peak forward displacements which can be attributed to the

increased adipose tissue volume around the hips. The muscle activation levels generated by the pre-crash manoeuvres were of similar magnitude between the HBMs, with some slight shifts to whether the left or right side had the highest muscle activation in the pre-crash braking due to the interaction with the shoulder belt.

The validation of the active F50 HBM and its application to whole-sequence crashes are initial steps towards FE HBMs which can represent the whole population of vehicle occupants in complex crash scenarios and be used to evaluate injury risk based on stresses and strains at tissue level. In the present study, however, injury predictions from the models were not assessed, as more work is needed to validate these from the morphed HBMs – work which is ongoing [47].

V. CONCLUSIONS

An average-sized female version of the active SAFER HBM version 10 was developed using mesh morphing and scaling of the active muscle cross-sectional area. The model was able to reproduce the postural response of average female volunteers during pre-crash manoeuvres, showing good biofidelity for occupant kinematics prediction in the pre-crash braking, and fair biofidelity in the evasive turning manoeuvres. Whole-sequence, pre-crash and in-crash simulations revealed some differences between the F50 and M50 models, with the F50 model showing lower upper body forward displacements, and higher pelvis displacements, regardless of crash configuration and belt system, which can be attributed to the difference in stature, mass, and adipose tissue. This study presents a promising step towards including the effects of physiological differences in occupant population in whole-sequence simulations to improve occupant safety. Future research may seek to investigate the effects of active musculature in occupant models on injury risks and in other types of crash scenarios

VI. ACKNOWLEDGEMENT

This work was carried out at SAFER, Vehicle and Traffic Safety Centre at Chalmers, Gothenburg, Sweden, and funded by FFI-Strategic Vehicle Research and Innovation, by Vinnova, the Swedish Energy Agency, the Swedish Transport Administration, and the Swedish vehicle industry. The simulations were enabled by resources provided by the National Academic Infrastructure for Supercomputing in Sweden (NAISS) at Chalmers partially funded by the Swedish Research Council through grant agreement no. 2022-06725.

VII. REFERENCES

[1] Forman, J., Poplin, G.S., et al. Automobile injury trends in the contemporary fleet: Belted occupants in frontal collisions. *Traffic injury prevention*, 2019. 20(6): p. 607-612

[2] Bose, D., Segui-Gomez, M., and Crandall, J.R. Vulnerability of female drivers involved in motor vehicle crashes: an analysis of US population at risk. *American journal of public health*, 2011. 101(12): p. 2368

[3] Kahane, C.J. Injury vulnerability and effectiveness of occupant protection technologies for older occupants and women. 2013: Report No: DOT HS 811 766, Washington, DC: National Highway Traffic Safety Administration.

[4] Brumbelow, M.L. and Jermakian, J.S. Injury risks and crashworthiness benefits for females and males: Which differences are physiological? *Traffic injury prevention*, 2022. 23(1): p. 11-16

[5] Östling, M., Lubbe, N., Jeppsson, H., and Puthan, P. Passenger car safety beyond ADAS: Defining remaining accident configurations as future priorities. *Proceedings of The 26th International Technical Conference on the Enhanced Safety of Vehicles, Eindhoven, Netherlands*, 2019.

[6] Seacrist, T., Sahani, R., et al. Efficacy of automatic emergency braking among risky drivers using counterfactual simulations from the SHRP 2 naturalistic driving study. *Safety science*, 2020. 128: p. 104746

[7] Tan, H., Zhao, F., et al. Automatic emergency braking (AEB) system impact on fatality and injury reduction in China. *International journal of environmental research and public health*, 2020. 17(3): p. 917

[8] Leledakis, A., Östh, J., Iraeus, J., Davidsson, J., and Jakobsson, L. The Influence of Occupant's Size, Shape and Seat Adjustment in Frontal and Side Impacts. *Proceedings of the International IRCOBI Conference*, 2019. Porto, Portugal

[9] Olafsdottir, J.M., Östh, J., Davidsson, J., and Brolin, K. Passenger kinematics and muscle responses in autonomous braking events with standard and reversible pre-tensioned restraints. *Proceedings of the International IRCOBI Conference*, 2013. Gothenburg, Sweden

[10] Kirschbichler, S., Huber, P., et al. Factors influencing occupant kinematics during braking and lane change maneuvers in a passenger vehicle. *Proceedings of the International IRCOBI conference*, 2014. Berlin, Germany

[11] Holt, C., Seacrist, T., et al. The effect of vehicle countermeasures and age on human volunteer kinematics during evasive swerving events. *Traffic injury prevention*, 2020. 21(1): p. 48-54

[12] Bose, D., Crandall, J.R., Untaroiu, C.D., and Maslen, E.H. Influence of pre-collision occupant parameters on injury outcome in a frontal collision. *Accident Analysis and Prevention*, 2010. 42(4): p. 1398-1407

[13] McMurry, T.L., Poplin, G.S., Shaw, G., and Panzer, M.B. Crash safety concerns for out-of-position occupant postures: A look toward safety in highly automated vehicles. *Traffic injury prevention*, 2018. 19(6): p. 582-587

[14] Nie, B., Sathyanarayan, D., Ye, X., Crandall, J.R., and Panzer, M.B. Active muscle response contributes to increased injury risk of lower extremity in occupant–knee airbag interaction. *Traffic injury prevention*, 2018. 19(sup1): p. S76-S82
[15] Carlsson, S. and Davidsson, J. Volunteer occupant kinematics during driver initiated and autonomous braking when driving in real traffic environments. *Proceedings of the international IRCOBI Conference*, 2011. Krakow, Poland
[16] Reed, M.P. Passenger Kinematics During Crash Avoidance Maneuvers. 2018, University of Michigan Transportation Research Institute: Report No: UMTRI-2018-5, Ann Arbor, MI, US.
[17] Reed, M.P., Ebert, S.M., Jones, M.H., and Park, B.-k.D. Occupant Dynamics During Crash Avoidance Maneuvers. 2021, University of Michigan Transportation Research Institute: Report No: UMTRI-2020-10, Ann Arbor, MI. US.
[18] Larsson, E., Ghaffari, G., Iraeus, J., and Davidsson, J. Passenger Kinematics Variance in Different Vehicle Manoeuvres–Biomechanical Response Corridors Based on Principal Component Analysis. *Proceedings of the international IRCOBI conference*, 2022. Porto, Portugal
[19] Reed, M.P., Ebert, S.M., et al. Passenger head kinematics in abrupt braking and lane change events. *Traffic injury prevention*, 2018. 19(sup2): p. S70-S77
[20] Maughan, R., Watson, J.S., and Weir, J. Strength and cross-sectional area of human skeletal muscle. *The Journal of physiology*, 1983. 338(1): p. 37-49
[21] Kanehisa, H., Ikegawa, S., and Fukunaga, T. Comparison of muscle cross-sectional area and strength between untrained women and men. *European journal of applied physiology and occupational physiology*, 1994. 68: p. 148-154
[22] Nuzzo, J.L. Narrative Review of Sex Differences in Muscle Strength, Endurance, Activation, Size, Fiber Type, and Strength Training Participation Rates, Preferences, Motivations, Injuries, and Neuromuscular Adaptations. *The Journal of Strength & Conditioning Research*, 2022: p. 10.1519
[23] Hwang, E., Hallman, J., et al. Rapid Development of Diverse Human Body Models for Crash Simulations through Mesh Morphing. 2016, SAE Technical Paper.
[24] Hwang, E., Hu, J., et al. Development, evaluation, and sensitivity analysis of parametric finite element whole-body human models in side impacts. *Proceedings of Stapp Car Crash Conference*, 2016. Washington, D.C.
[25] Beillas, P. and Berthet, F. An investigation of Human Body Model morphing for the assessment of abdomen responses to impact against a population of test subjects. *Traffic injury prevention*, 2017. 18(sup1): p. S142-S147
[26] Shigeta, K., Kitagawa, Y., and Yasuki, T. Development of next generation human FE model capable of organ injury prediction. *Proceedings of The 21st Annual Enhanced Safety of Vehicles*, 2009. Stuttgart, Germany
[27] Gayzik, F.S., Moreno, D.P., Vavalle, N.A., Rhyne, A.C., and Stitzel, J.D. Development of a full human body finite element model for blunt injury prediction utilizing a multi-modality medical imaging protocol. *Proceedings of 12th International LS-DYNA User Conference*, 2012. Koblenz, Germany
[28] Pipkorn, B., Östh, J., et al. Validation of the SAFER Human Body Model Kinematics in Far-Side Impacts. *Proceedings of the International IRCOBI Conference*, 2021. Online
[29] John, J., Klug, C., Kranjec, M., Svenning, E., and Iraeus, J. Hello, world! VIVA+: A human body model lineup to evaluate sex-differences in crash protection. *Frontiers in bioengineering and biotechnology*, 2022. 10
[30] Kato, D., Nakahira, Y., Atsumi, N., and Iwamoto, M. Development of human-body model THUMS Version 6 containing muscle controllers and application to injury analysis in frontal collision after brake deceleration. *Proceedings of Proceedings of the IRCOBI Conference, Athens, Greece*, 2018.
[31] Devane, K., Johnson, D., and Gayzik, F.S. Validation of a simplified human body model in relaxed and braced conditions in low-speed frontal sled tests. *Traffic injury prevention*, 2019. 20(8): p. 832-837
[32] Larsson, E., Iraeus, J., et al. Active human body model predictions compared to volunteer response in experiments with braking, lane change, and combined manoeuvres. *Proceedings of the International IRCOBI Conference*, 2019. Florence, Italy
[33] Devane, K., Chan, H., Albert, D., Kemper, A., and Gayzik, F.S. Implementation and calibration of active small female and average male human body models using low-speed frontal sled tests. *Traffic injury prevention*, 2022: p. 1-6
[34] Mishra, A., Ghosh, P., Chitteti, R., and Mayer, C. Development of a Chinese 5th percentile female active human body model. *Hip*, 2020. 1(6): p. 17
[35] Behr, M., Arnoux, P.-J., Serre, T., Thollon, L., and Brunet, C. Tonic finite element model of the lower limb. *Journal of Biomechanical Engineering*, 2006. 128: p. 223-228
[36] Sugiyama, T., Kimpara, H., et al. Effects of muscle tense on impact responses of lower extremity. *Proceedings of the international IRCOBI Conference*, 2007. Maastricht, The Netherlands
[37] Chang, C.Y., Rupp, J.D., Kikuchi, N., and Schneider, L.W. Development of a finite element model to study the effects of muscle forces on knee-thigh-hip injuries in frontal crashes. *Stapp car crash journal*, 2008. 52: p. 475-504
[38] Chang, C.Y., Rupp, J.D., Reed, M.P., Hughes, R.E., and Schneider, L.W. Predicting the effects of muscle activation on knee, thigh, and hip injuries in frontal crashes using a finite-element model with muscle forces from subject testing and musculoskeletal modeling. *Stapp car crash journal*, 2009. 53: p. 291-328
[39] Iwamoto, M., Nakahira, Y., and Sugiyama, T. Investigation of pre-impact bracing effects for injury outcome using an active human FE model with 3D geometry of muscles. *Proceedings of the 22nd international technical conference on the enhanced safety of vehicles (ESV)*, 2011. Washington, DC, USA
[40] González-García, M., Weber, J., and Peldschus, S. Potential effect of pre-activated muscles under a far-side lateral impact. *Traffic Injury Prevention*, 2021. 22(sup1): p. S148-S152

[41] Östh, J., Larsson, E., and Jakobsson, L. Human Body Model Muscle Activation Influence on Crash Response. *Proceedings of the International IRCOBI Conference*, 2022. Porto, Portugal
[42] Ólafsdóttir, J., Östh, J., and Brolin, K. Modelling Reflex Recruitment of Neck Muscles in a Finite Element Human Body Model for Simulating Omnidirectional Head Kinematics. *Proceedings of the International IRCOBI Conference*, 2019. Florence, Italy
[43] Iraeus, J. and Pipkorn, B. Development and Validation of a Generic Finite Element Ribcage to be used for Strain-based Fracture Prediction. *Proceedings of 2019 International IRCOBI Conference,*, 2019. Athens, Greece
[44] Pipkorn, B., Iraeus, J., Bjorklund, M., Bunketorp, O., and Jakobsson, L. Multi-Scale validation of a rib fracture prediction method for human body models. *Proceedings of the International IRCOBI Conference*, 2019. Online
[45] Kleiven, S. Predictors for traumatic brain injuries evaluated through accident reconstructions. *Stapp car crash journal*, 2007. 51: p. 81-114
[46] Schneider, L. Development of anthropometrically based design specifications for an advanced adult anthropomorphic dummy family, volume 1. final report. 1983: Report No: UMTRI-83-53-1, Ann Arbour, MI, US.
[47] Larsson, K.-J., Pipkorn, B., Iraeus, J., Forman, J., and Hu, J. Evaluation of a diverse population of morphed human body models for prediction of vehicle occupant crash kinematics. *Computer Methods in Biomechanics and Biomedical Engineering*, 2021: p. 1-31
[48] Vasavada, A.N., Danaraj, J., and Siegmund, G.P. Head and neck anthropometry, vertebral geometry and neck strength in height-matched men and women. *Journal of biomechanics*, 2008. 41(1): p. 114-121
[49] Zheng, L., Siegmund, G., Ozyigit, G., and Vasavada, A. Sex-specific prediction of neck muscle volumes. *Journal of biomechanics*, 2013. 46(5): p. 899-904
[50] Valera-Calero, J.A., Gallego-Sendarrubias, G., et al. Cross-sectional area of the cervical extensors assessed with panoramic ultrasound imaging: Preliminary data in healthy people. *Musculoskeletal Science and Practice*, 2020. 50: p. 102257
[51] Ghaffari, G., Brolin, K., et al. Passenger kinematics in Lane change and Lane change with Braking Manoeuvres using two belt configurations: standard and reversible pre-pretensioner. *Proceedings of the International IRCOBI Conference*, 2018. Athens, Greece
[52] Ghaffari, G. and Davidsson, J. Female kinematics and muscle responses in lane change and lane change with braking maneuvers. *Traffic injury prevention*, 2021. 22(3): p. 236-241
[53] Davidsson, J. Validated and Computationally Robust Active HBMs, in *OSCCAR: Future Occupant Safety For Crashes In Cars deliverable D 3.2*. 2021. p. 27-28.
[54] Gehre, C., Gades, H., and Wernicke, P. Objective rating of signals using test and simulation responses. *Proceedings of The 21st Annual Enhanced Safety of Vehicles*, 2009. Stuttgart, Germany
[55] Thunert, C. CORA Release 4.0.4 User's Manual. 2017, PDB - Partnership for Dummy Technology and Biomechanics: Gaimersheim, Germany.
[56] Östh, J., Ólafsdóttir, J.M., Davidsson, J., and Brolin, K. Driver kinematic and muscle responses in braking events with standard and reversible pre-tensioned restraints: validation data for human models. *Stapp car crash journal*, 2013. 57: p. 1
[57] Poulard, D., Subit, D., Donlon, J.-P., and Kent, R.W. Development of a computational framework to adjust the pre-impact spine posture of a whole-body model based on cadaver tests data. *Journal of biomechanics*, 2015. 48(4): p. 636-643
[58] Reed, M.P. and Ebert, S.M. Elderly occupants: posture, body shape, and belt fit. 2013: Report No: UMTRI-2013-26, Ann Arbor, MI, US.
[59] Wang, Y., Cao, L., et al. A parametric ribcage geometry model accounting for variations among the adult population. *Journal of Biomechanics*, 2016. 49(13): p. 2791-2798
[60] Klein, K.F. Use of Parametric Finite Element Models to Investigate Effects of Occupant Characteristics on Lower-Extremity Injuries in Frontal Crashes, in *Department of Biomedical Engineering*. 2015, University of Michigan.
[61] Klein, K.F., Hu, J., Reed, M.P., Hoff, C.N., and Rupp, J.D. Development and validation of statistical models of femur geometry for use with parametric finite element models. *Annals of biomedical engineering*, 2015. 43(10): p. 2503-2514
[62] Agnew, A.M., Murach, M.M., et al. Sources of Variability in Structural Bending Response of Pediatric and Adult Human Ribs in Dynamic Frontal Impacts. *Stapp Car Crash Journal*, 2018. 62: p. 119-192
[63] Holcombe, S.A. and Derstine, B.A. Rib cortical bone thickness variation in adults by age and sex. *Journal of Anatomy*, 2022. 241(6): p. 1344-1356
[64] Katzenberger, M.J., Albert, D.L., Agnew, A.M., and Kemper, A.R. Effects of sex, age, and two loading rates on the tensile material properties of human rib cortical bone. *Journal of the Mechanical Behavior of Biomedical Materials*, 2019. 102: p. 103410
[65] Chandrashekar, N., Mansouri, H., Slauterbeck, J., and Hashemi, J. Sex-based differences in the tensile properties of the human anterior cruciate ligament. *Journal of biomechanics*, 2006. 39(16): p. 2943-2950
[66] Pipkorn, B., Larsson, K.-J., et al. Occupant Protection in Far-Side Impacts. *Proceedings of the international IRCOBI Conference*, 2017. Athens, Greece
[67] Foust, D.R., Chaffin, D.B., Snyder, R.G., and Baum, J.K. Cervical range of motion and dynamic response and strength of cervical muscles. *SAE Transactions*, 1973: p. 3222-3234
[68] Östh, J., Eliasson, E., Happee, R., and Brolin, K. A method to model anticipatory postural control in driver braking events. *Gait & posture*, 2014. 40(4): p. 664-669

VIII. APPENDIX

Mesh quality

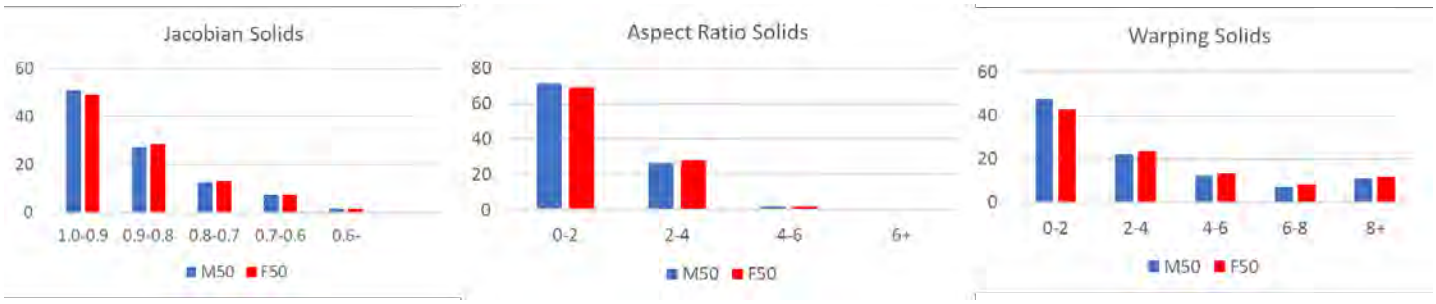

Fig. A 1. Comparison of mesh quality of active M50 and F50 models

CORA Settings

TABLE A 1
CORA SETTINGS

Setting	Weight
Corridor rating	0.5
Cross-correlation rating	0.5
Shape	0.5
Size	0.25
Phase-shift	0.25

Detailed Validation Results

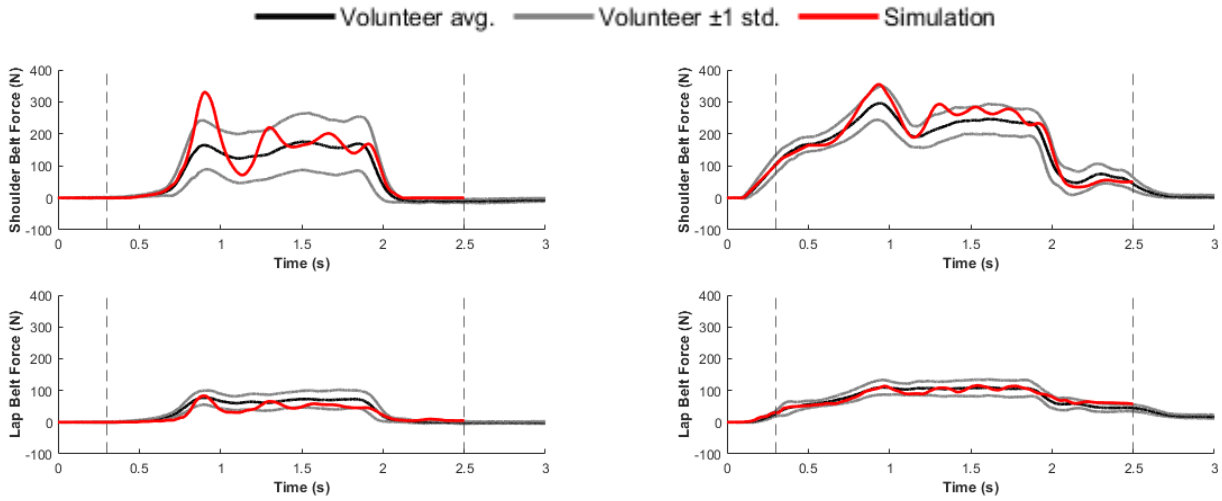

(a) Standard seatbelt (b) ERR seatbelt

Fig. A 2. Seatbelt forces for pre-crash braking simulations with (a) standard seatbelt and (b) ERR seatbelt. The black curves show the average F50 volunteer response, grey curves show the average ±1 SDs, and the red curves show active F50 HBM response. The vertical dashed lines show the evaluation interval.

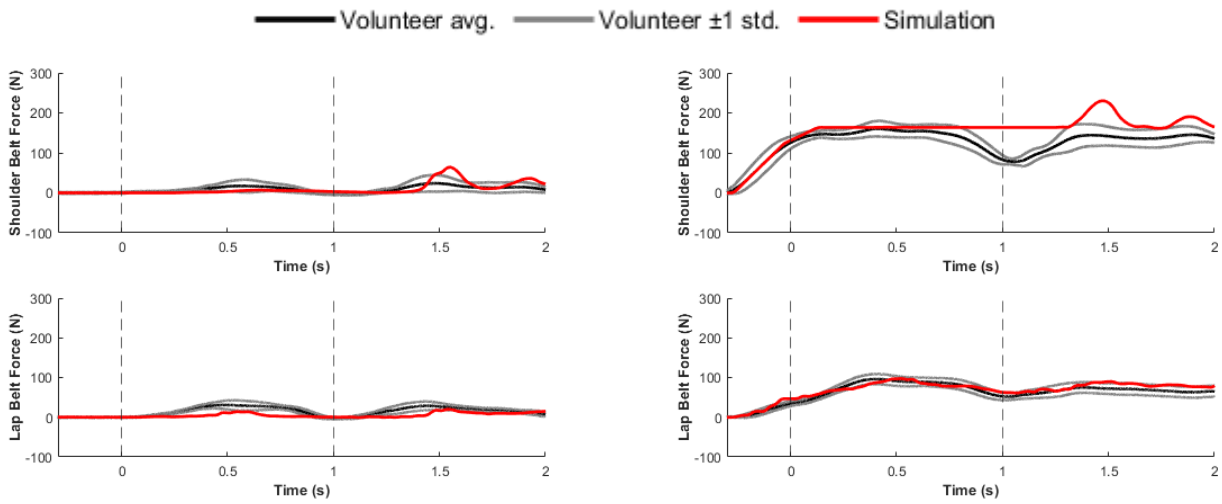

(a) Standard seatbelt (b) ERR seatbelt

Fig. A 3. Seatbelt forces for evasive turning simulations with (a) standard seatbelt and (b) ERR seatbelt. The black curves show the average F50 volunteer response, grey curves show the average ±1 SDs, and the red curves show active F50 HBM response. The vertical dashed lines show the evaluation interval.

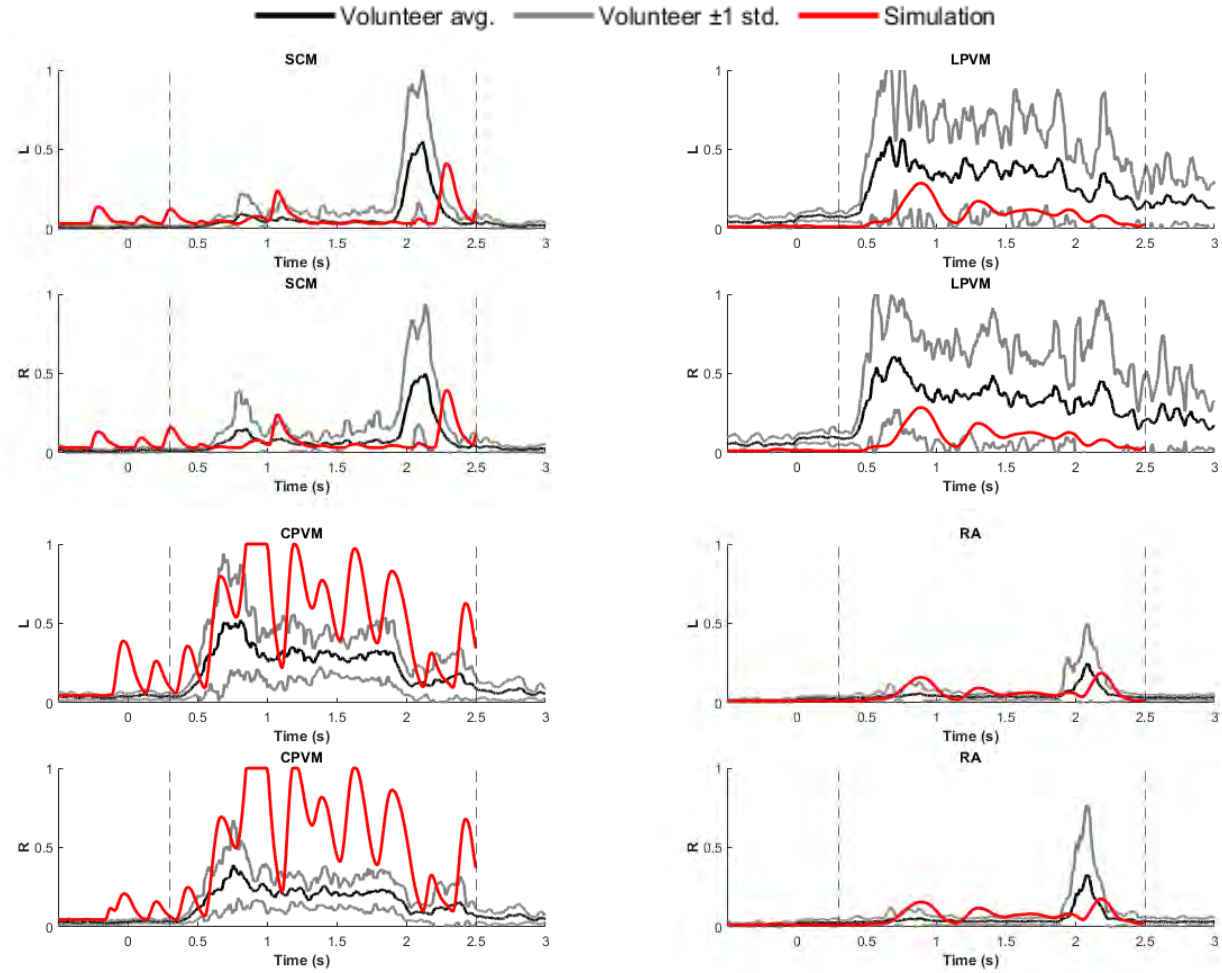

Fig. A 4. Muscle activations in pre-crash braking with standard seatbelt. The black curves show the average F50 volunteer response, grey curves show the average ±1 SDs, and the red curves show the active F50 HBM response. The vertical dashed lines show the evaluation interval.

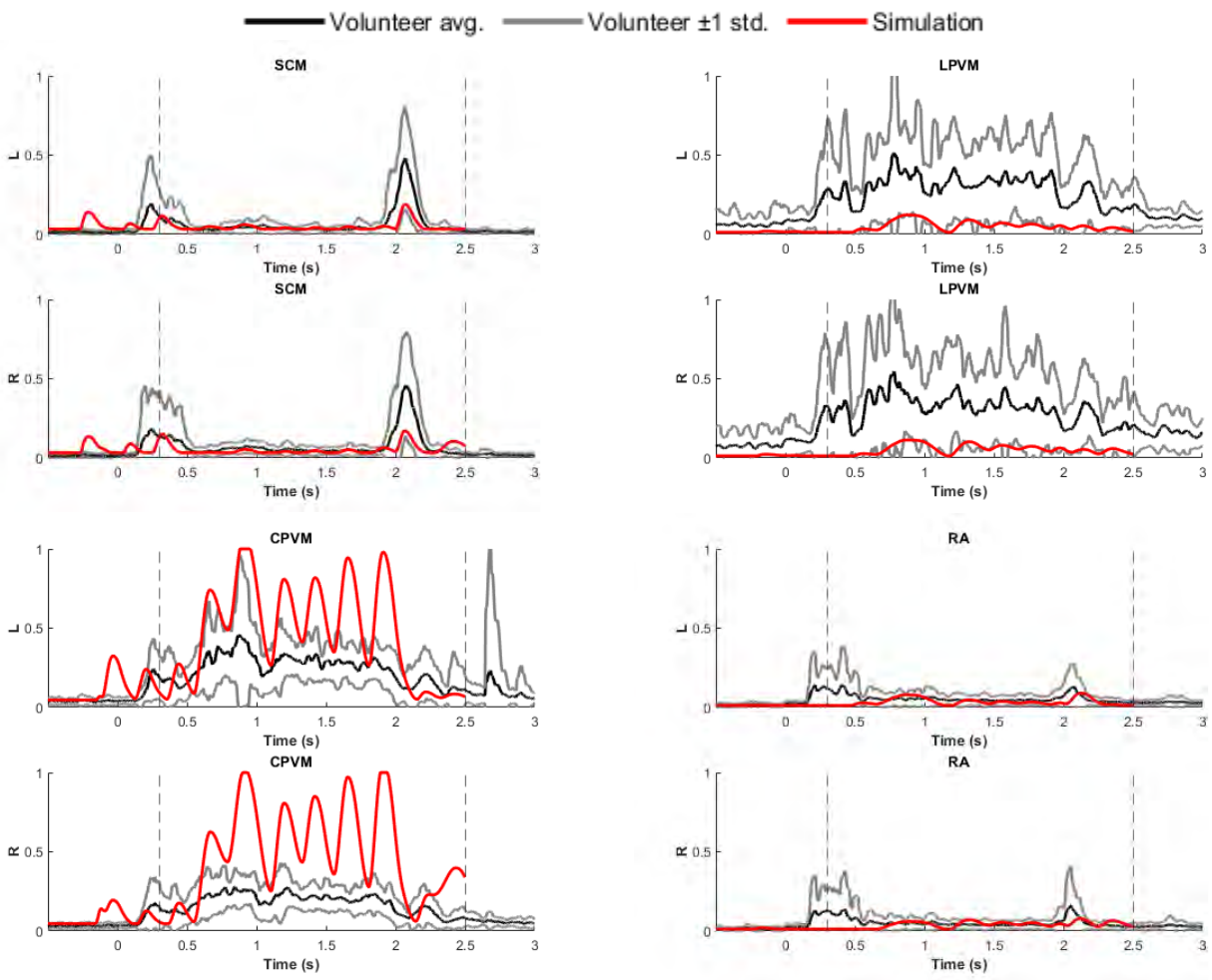

Fig. A 5. Muscle activations in pre-crash braking with ERR seatbelt. The black curves show the average F50 volunteer response, grey curves show the average ±1 SDs, and the red curves show the active F50 HBM response. The vertical dashed lines show the evaluation interval.

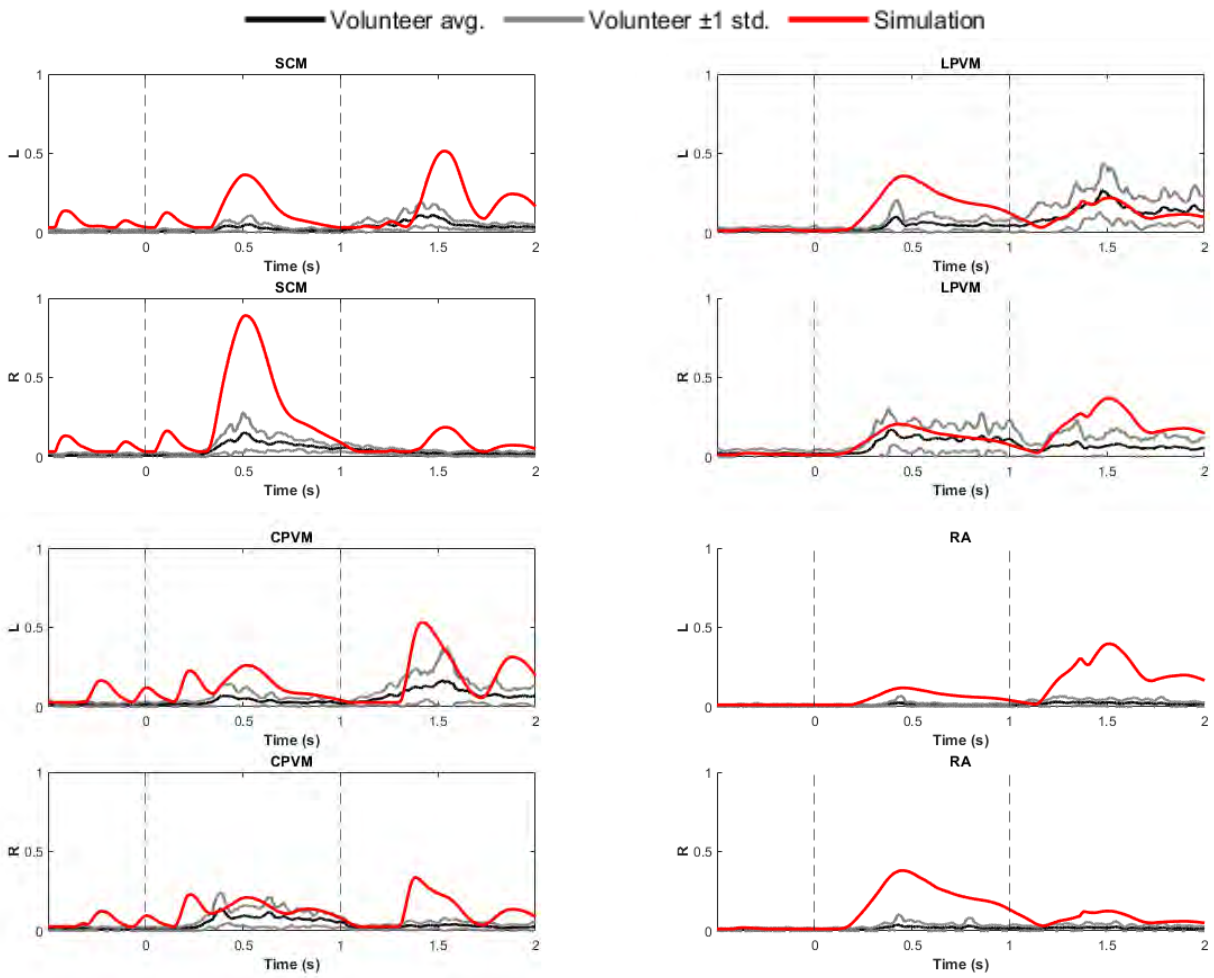

Fig. A 6. Muscle activations in evasive turning with standard seatbelt. The black curves show the average F50 volunteer response, grey curves show the average ±1 SDs, and the red curves show the active F50 HBM response. The vertical dashed lines show the evaluation interval.

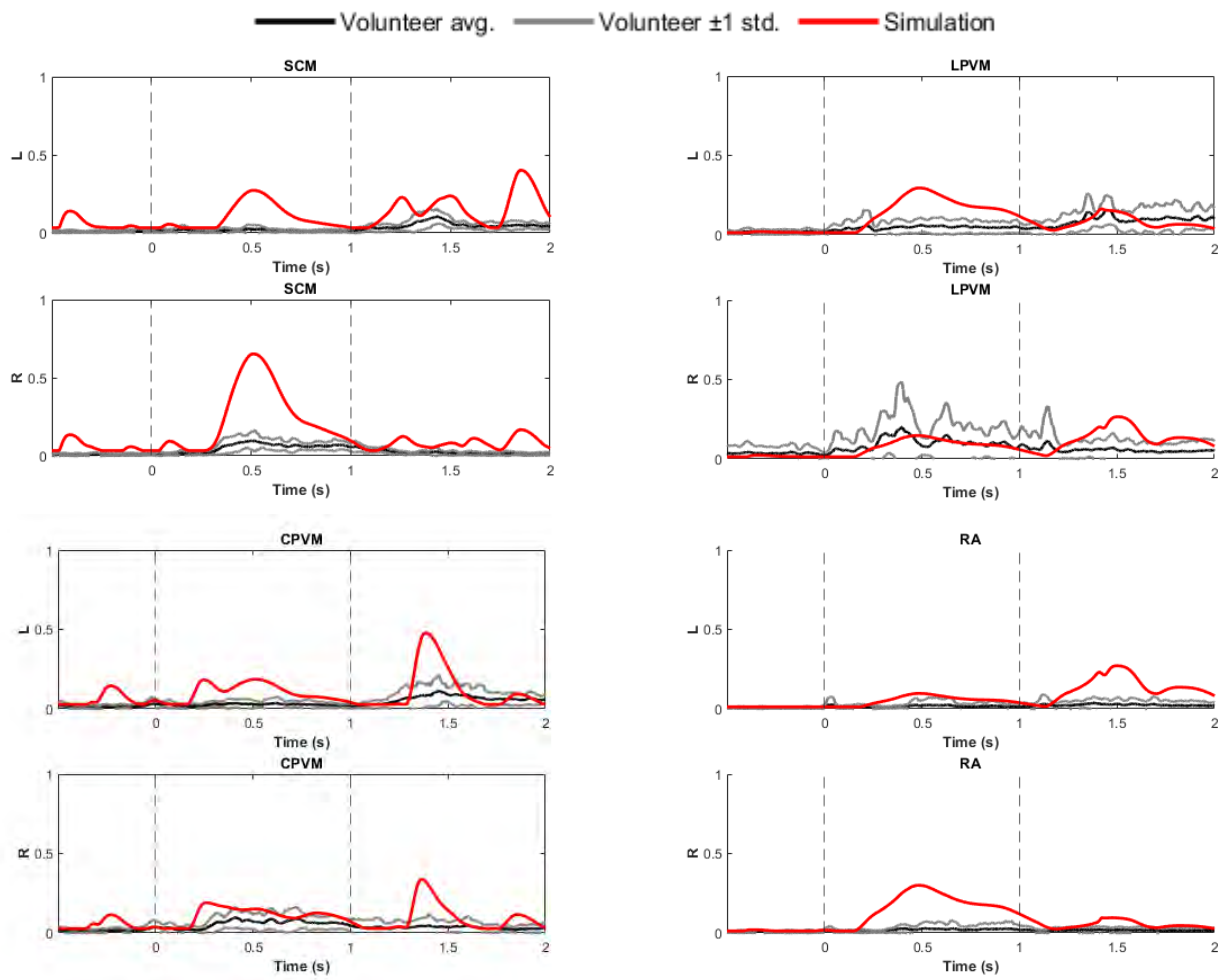

Fig. A 7. Muscle activations in evasive turning with ERR seatbelt. The black curves show the average F50 volunteer response, grey curves show the average ±1 SDs, and the red curves show the active F50 HBM response. The vertical dashed lines show the evaluation interval.

SAFER HBM Muscle Spatial Tuning Groups

The muscle activation for the SAFER HBM were calculated for eight spatial tuning groups for the cervical controller (Fig. A 8) and for four groups for the lumbar controller (Fig. A 9). All the muscles in each group, on the same side of the sagittal midplane of the body had the same activation level and resulting muscle activation in the simulation which were presented and analysed in these groups.

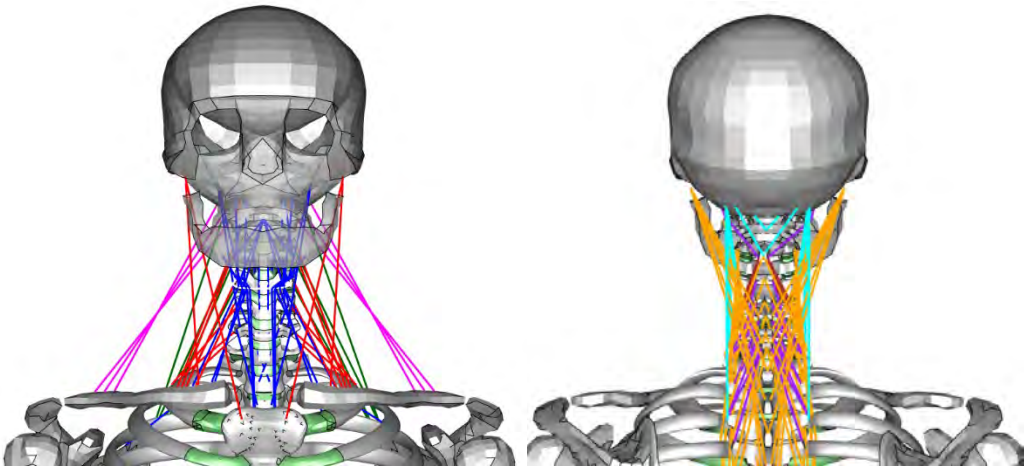

Fig. A 8. Cervical muscle spatial tuning groups. Red: Sternocleidomastoideus (SCM) group. Blue: Sternohyoid (STH) group. Green: Levator Scapulae (LS) group. Magenta: Trapezius (TRAP) group. Cyan: Semispinalis Capitis (SCap) group. Orange: Semispinalis Cervicis (SCerv) group. Brown: C4 level Multifidus (CM-C4) group. Purple: C6 level Multifidus (CM-C6) group.

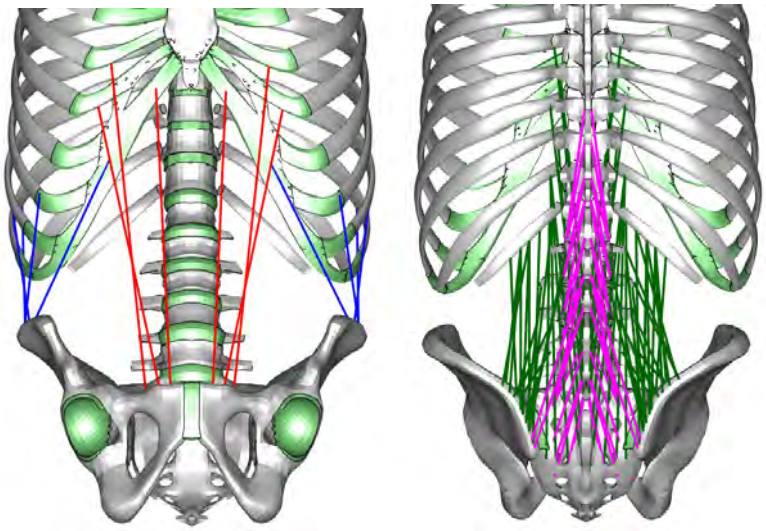

Fig. A 9. Lumbar muscle spatial tuning groups. Red: Rectus Abdominis (RA) group. Blue: Obliques (OBL) group. Green: Lumbar Erector Spinae (LES) group. Magenta: Lumbar Multifidus group (LMF).

Occupant Compartment Model for Whole-Sequence Simulations

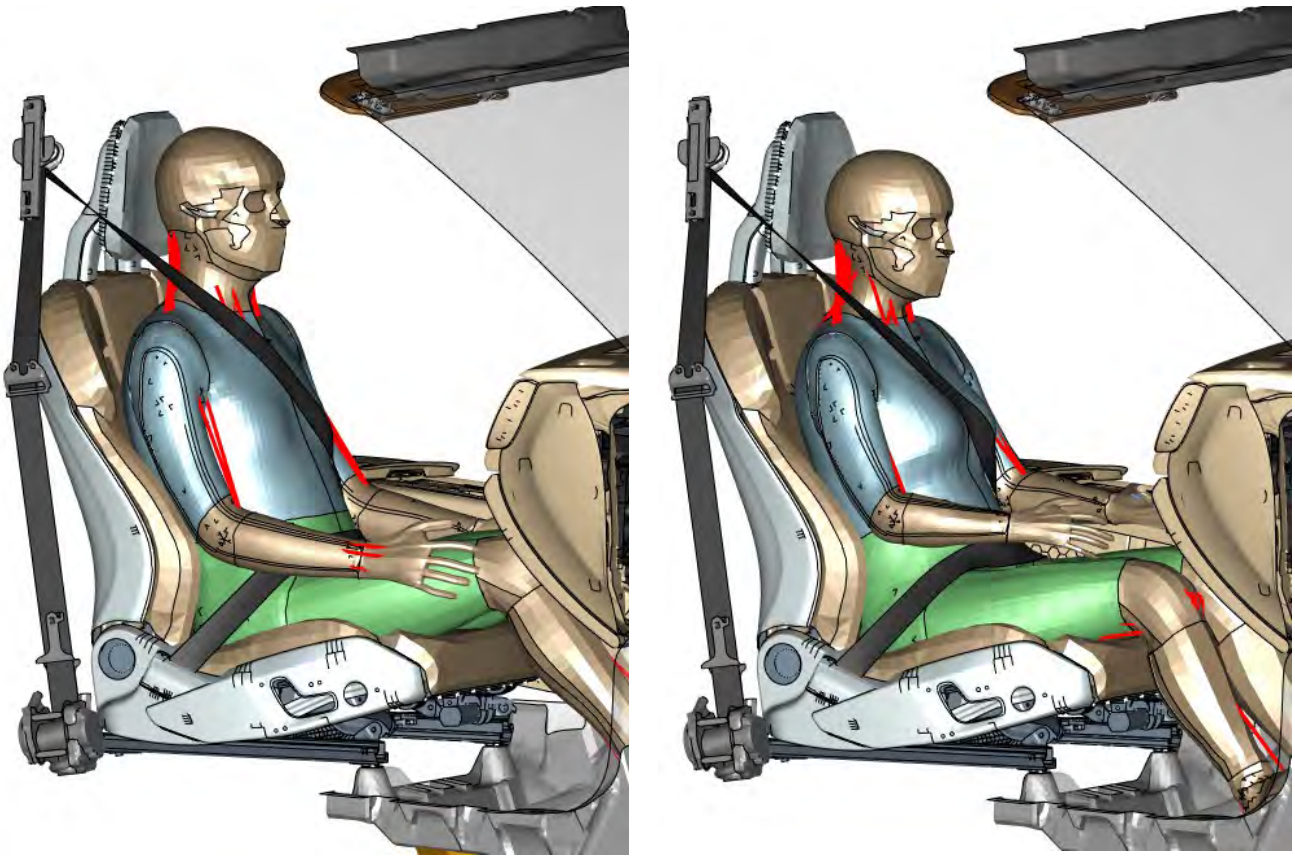

Fig. A 10. HBMs in the occupant compartment model used for whole-sequence crash simulations. Left: Active SAFER HBM M50. Right: Active SAFER HBM F50.

Muscle Activations during the Pre-Crash Phase

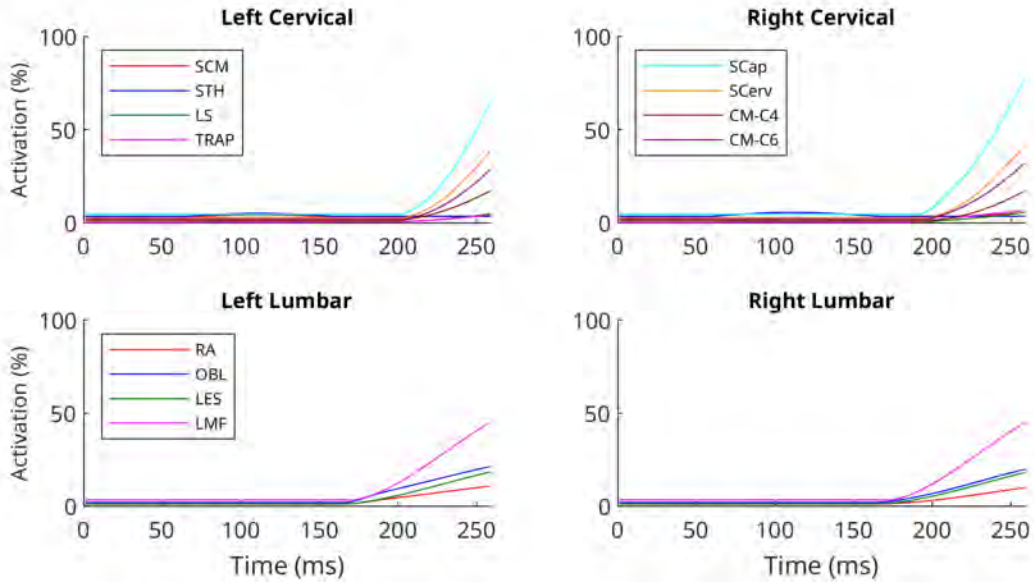

Fig. A 11. M50 muscle activation time histories during the pre-crash braking in Simulation 3. Muscle group abbreviations according to Fig. A 8 and Fig. A 9.

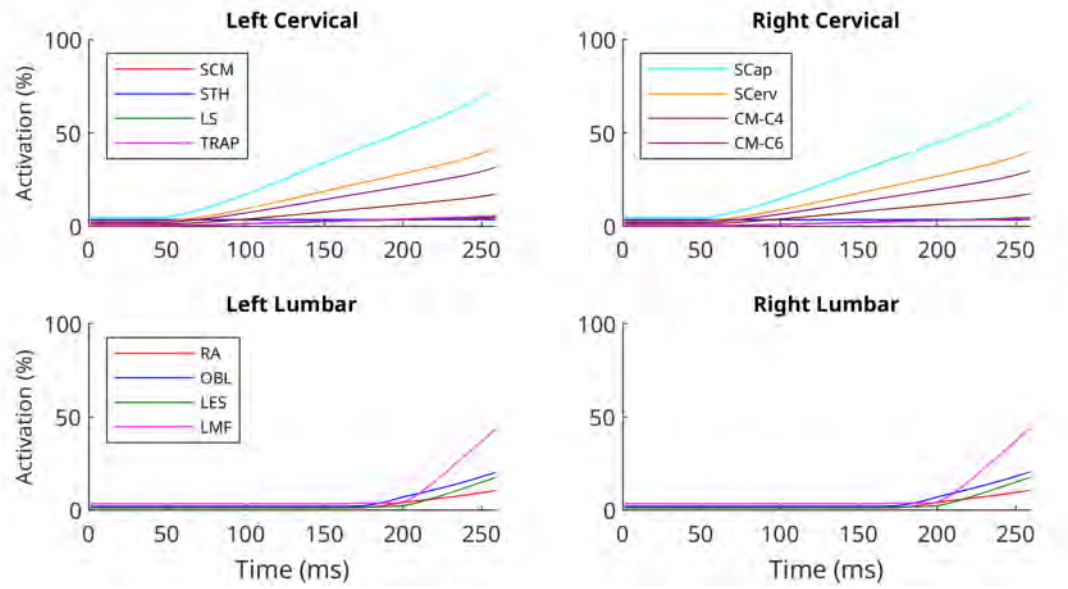

Fig. A 12. F50 muscle activation time histories during the pre-crash braking in Simulation 4. Muscle group abbreviations according to Fig. A 8 and Fig. A 9.

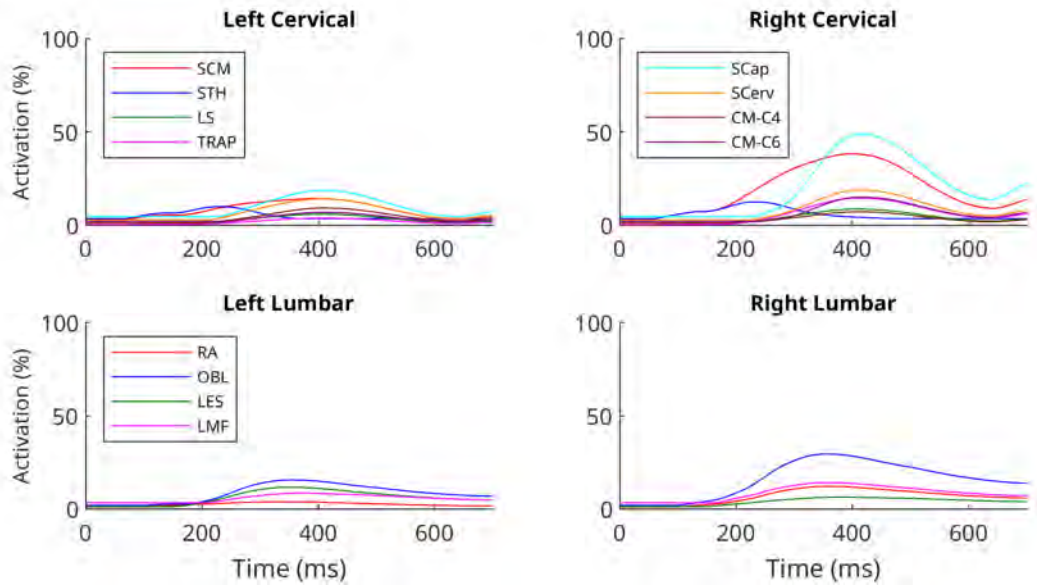

Fig. A 13. M50 muscle activation time histories during the pre-crash right turn in Simulation 15. Muscle group abbreviations according to according to Fig. A 8 and Fig. A 9.

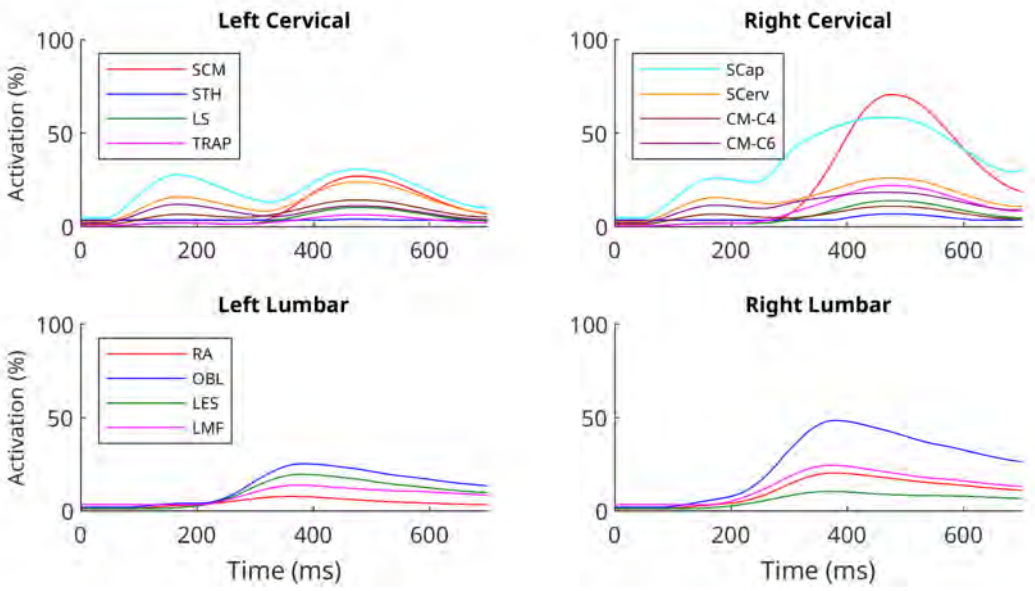

Fig. A 14. F50 muscle activation time histories during the pre-crash right turn in Simulation 16. Muscle group abbreviations according to Fig. A 8 and Fig. A 9.

HBM Crash Kinematics Snapshots

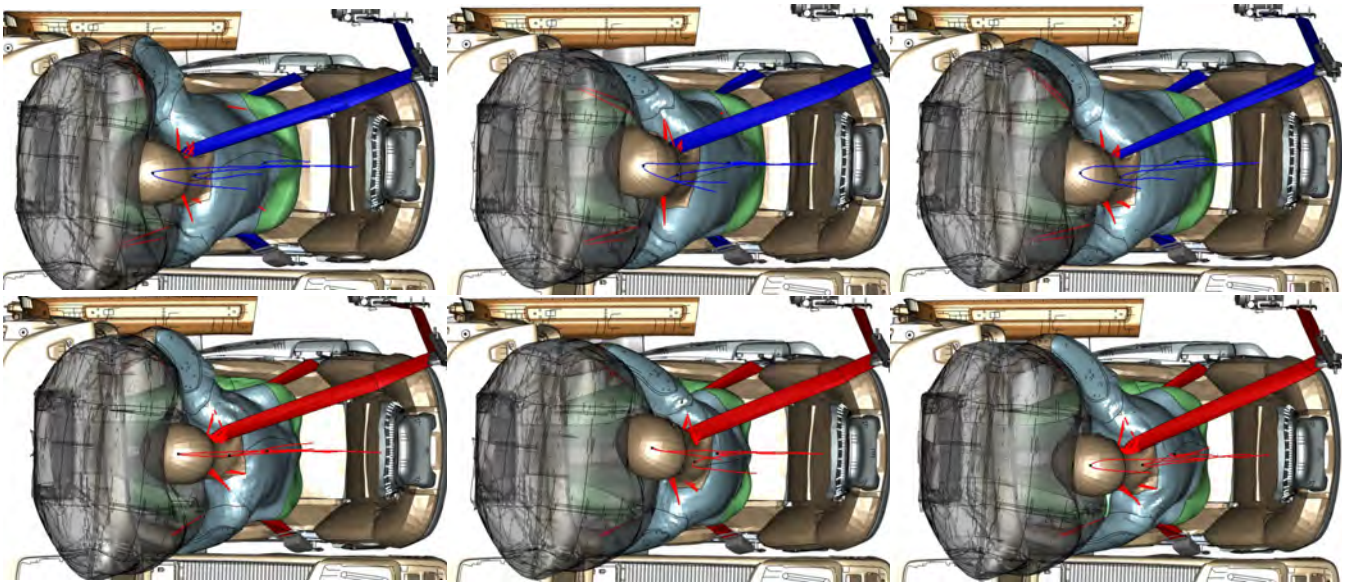

Fig. A 15. Snapshots of the HBMs at peak forward head displacements during the crash phase for Simulation 1–6. Top row: Simulation 1, 3 and 5 with the M50 HBM, from left to right. Bottom row: Simulation 2, 4 and 6 with the active F50 HBM, from left to right. Trajectories of head, T1 and sacrum from the whole-sequence simulation shown.

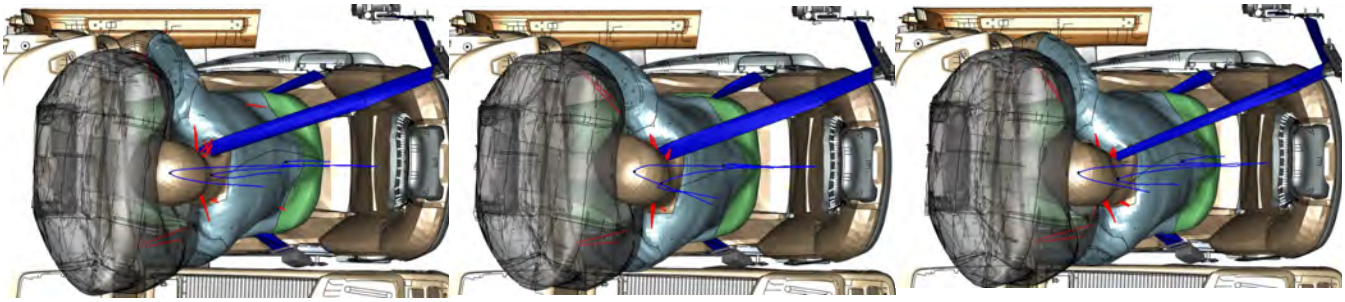

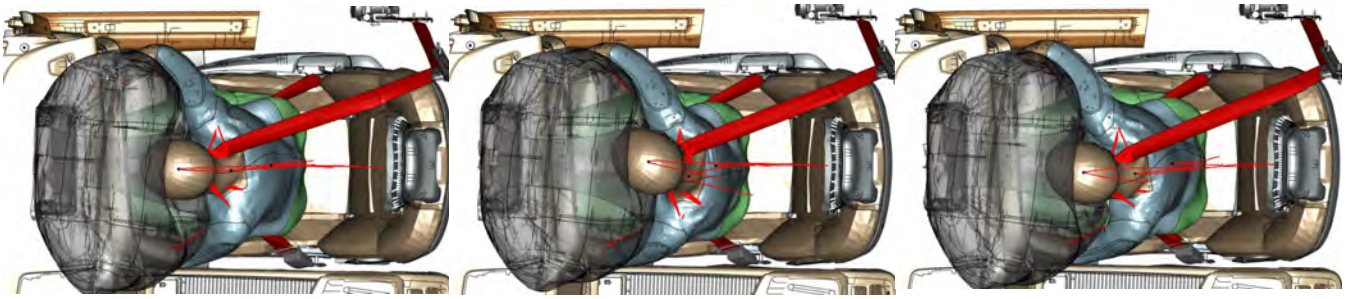

Fig. A 16. Snapshots of the HBMs at peak forward head displacements during the crash phase for Simulation 7–12. Top row: Simulation 7, 9 and 11 with the M50 HBM, from left to right. Bottom row: Simulation 8, 10 and 12 with the active F50 HBM, from left to right. Trajectories of head, T1 and sacrum from the whole-sequence simulation shown.

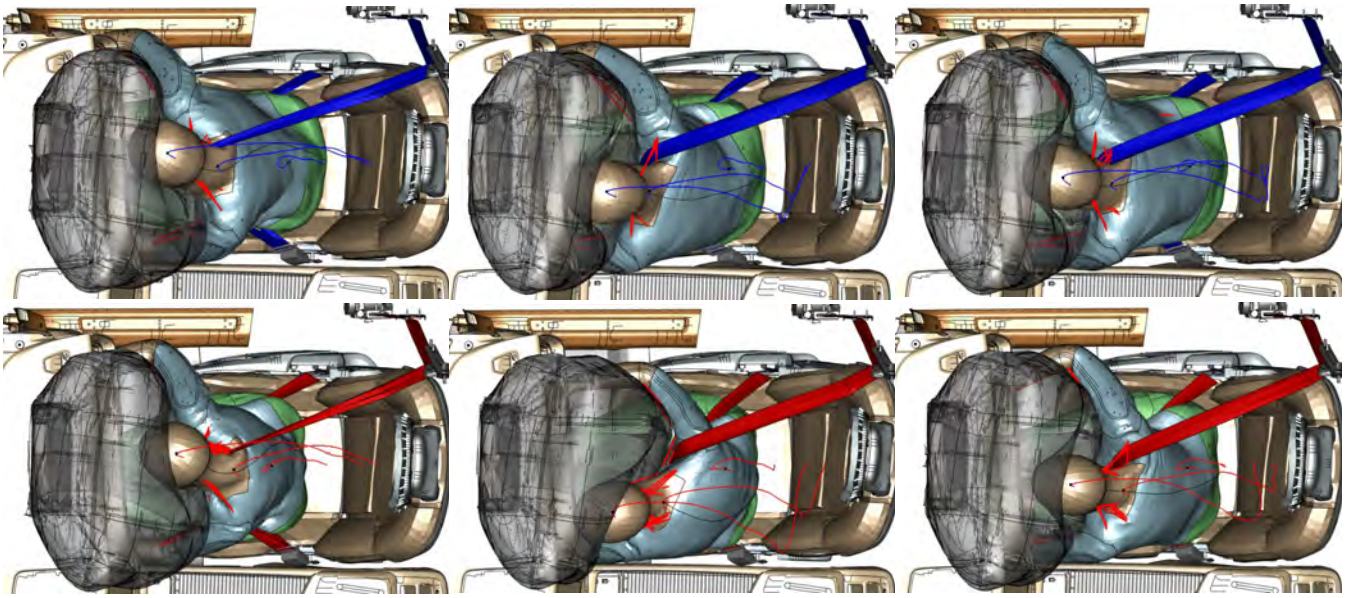

Fig. A 17. Snapshots of the HBMs at peak forward head displacements during the crash phase for Simulation 13–18. Top row: Simulation 13, 15 and 17 with the M50 HBM, from left to right. Bottom row: Simulation 14, 16 and 18 with the active F50 HBM, from left to right. Trajectories of head, T1 and sacrum from the whole-sequence simulation shown.

Differences in Soft Tissue Distribution

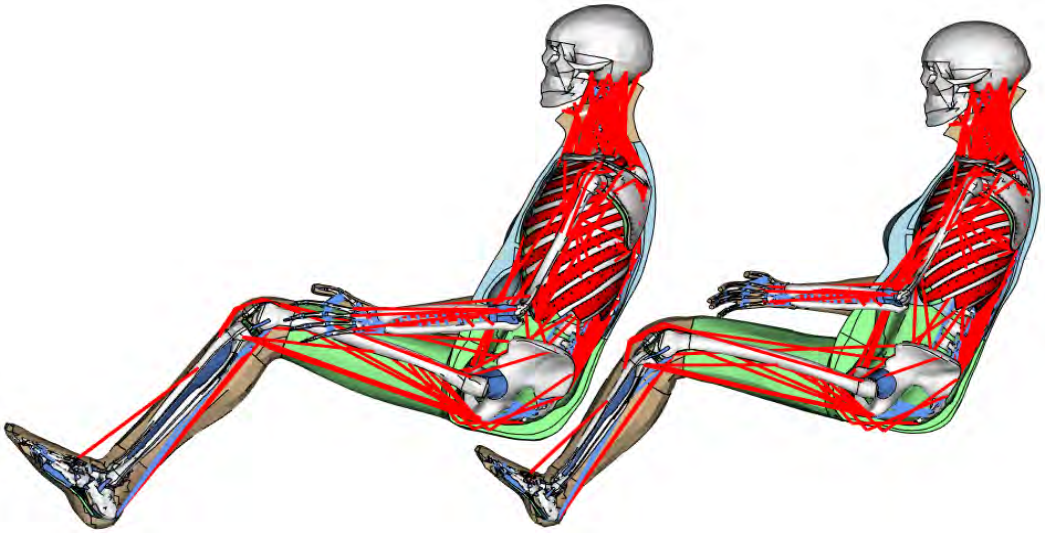

Fig. A 18. Difference in soft tissue distribution between the average male (left) and the average female (right) models.